Research Square

Preprints are preliminary reports that have not undergone peer review.
They should not be considered conclusive, used to inform clinical practice,
or referenced by the media as validated information.

Thermal Bridging and Energy Performance of Facade Columns

Raúl-Tomás Mora-García
University of Alicante
María-Francisca Céspedes-López
paqui.cespedes@ua.es
University of Alicante
Raúl Pérez-Sánchez
University of Alicante
Juan-Carlos Pérez-Sánchez
University of Alicante

Research Article

Keywords: Thermal bridging, building thermal modeling, facade columns, parametric simulation, building envelope, linear thermal transmittance

Posted Date: June 18th, 2026

DOI: https://doi.org/10.21203/rs.3.rs-9823147/v1

License: This work is licensed under a Creative Commons Attribution 4.0 International License.
Read Full License

Additional Declarations: No competing interests reported.

Thermal Bridging and Energy Performance of Facade Columns

Raúl-Tomás Mora-García[1]; María-Francisca Céspedes-López[1,2]; Raúl Pérez-Sánchez[1]; Juan-Carlos Pérez-Sánchez[1]

[1] Universidad de Alicante, Carretera San Vicente del Raspeig s/n, 0369 San Vicente del Raspeig Alicante (Spain).

[2] Corresponding author: paqui.cespedes@ua.es.

Abstract

Reinforced concrete columns embedded in facade walls may act as significant thermal bridges, reducing the effectiveness of envelope improvement measures in existing residential buildings. This study evaluates the effect of column-induced thermal bridges in two common Spanish facade typologies under internal retrofit scenarios. A parametric database of 1,710 construction solutions was generated by varying column position, insulation continuity, insulation location relative to the column, insulation thickness, insulation thermal conductivity, and the presence of an unventilated air cavity. Linear thermal transmittance was calculated using two-dimensional finite-element modeling, and the relative influence of the design variables was assessed using Ordinary Least Squares and Quantile Regression. The results show that insulation continuity at the column is the most influential factor in reducing linear thermal transmittance, followed by insulation position and insulation thickness. The findings provide design-oriented evidence for improving facade thermal performance and highlight the need to address structural thermal bridges in both retrofit and new-construction contexts.

Keywords: Thermal bridging; building thermal modeling; facade columns; parametric simulation; building envelope; linear thermal transmittance.

1. Introduction

Thermal bridges are critical weak points in the building envelope because they locally increase heat transfer and may significantly affect overall building energy performance. Their effect becomes more pronounced as envelope insulation improves, since non-uniform heat transfer through junctions accounts for a larger share of total transmission losses. For this reason, the accurate assessment of thermal bridges is essential for improving facade design, envelope performance, and the energy behavior of buildings. In this context, facade-integrated structural elements deserve particular attention because they may interrupt thermal continuity and reduce the effectiveness of construction solutions aimed at enhancing building performance [1-5].

To address this issue, the European Union has enacted several directives aimed at improving the energy efficiency of the building stock and reducing greenhouse gas emissions. In Spain, these directives are transposed through the Technical Building Code (CTE), which establishes the basic quality requirements for buildings. More specifically, the Basic Document on Energy Saving (DB-HE) defines the energy performance requirements and parameters that buildings must satisfy in order to align with the European decarbonization objectives for the sector [6-9].

In Spain, this issue is particularly important because a large share of the residential stock was built before current energy-efficiency requirements came into force. According to national housing stock data, approximately 53% of existing dwellings were built before 1980, when no regulatory requirements on energy efficiency were in place, while only a limited share was built under the current Technical Building Code framework (Figure 1). As a result, a large

part of the Spanish residential stock still shows low thermal performance and requires retrofit interventions to reduce energy demand and align with current decarbonization targets [6, 7, 10, 11].

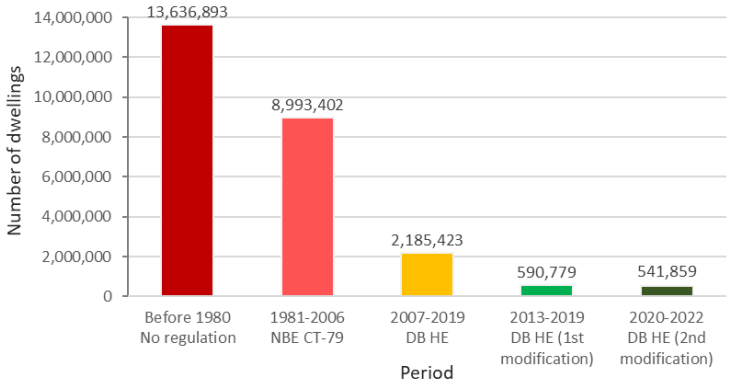


Figure 1. Number of dwellings classified by year of construction and applicable energy regulation. Source: Author's own creation based on data from INE [11] and Ministerio de Transportes [12].

The current regulatory framework places particular emphasis on energy losses through thermal bridges, which are defined as areas of the building envelope where variations in construction uniformity occur. Such non-uniformity may result from changes in material thermal conductivity, wall thickness, or geometric discontinuities between interior and exterior elements, such as those occurring at junctions between walls, floors, and ceilings [8, 9]. In this regard, compliance with the requirements of DB-HE in retrofit interventions requires particular attention to the treatment of thermal bridges.

External Thermal Insulation Composite Systems (ETICS) are increasingly used in Spain as an effective strategy for building energy retrofit because they mitigate thermal bridges at the junctions between structural elements and enclosures, improve thermal continuity, and reduce heat losses through the envelope. Nevertheless, despite their advantages, ETICS are not always feasible. In buildings under horizontal property regimes, facade rehabilitation requires agreement among all owners. In buildings with heritage protection affecting facade elements, ETICS cannot be applied because it alters the original state of the protected features. Under these conditions, interventions from the interior side of the facade become a practical alternative [2, 13, 14].

Public administrations have attempted to support this process through both regulation and financial incentives. On the one hand, the legal framework requires property owners to maintain and rehabilitate buildings. On the other hand, several public programs and fiscal measures have been implemented to encourage investment in energy retrofit (Figure 2). These mechanisms have enabled a substantial number of dwellings to apply for and receive rehabilitation support. Although this study does not focus on policy assessment, this context helps explain why facade retrofit and its technical feasibility have become increasingly relevant in the Spanish residential sector [15-24].

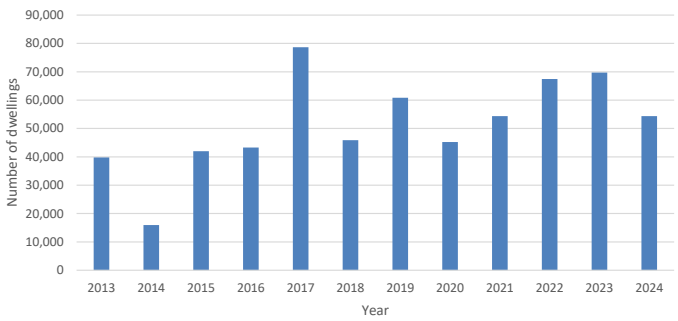


Figure 2. Number of protected dwellings receiving final approval for rehabilitation aid (national and regional). Source: Author's own creation based on data from Ministerio de Transportes [25].

As an alternative to ETICS, energy retrofit can be carried out from the interior side of the facade. However, this approach presents significant challenges, including the reduction of usable indoor space and the presence of reinforced concrete columns integrated into the envelope, which generate numerous thermal bridges. In these cases, the improvement of wall thermal transmittance does not necessarily eliminate the thermal penalty associated with structural junctions, and unresolved columns may continue to compromise facade thermal performance.

This study examines the thermal-bridge effect of reinforced concrete columns embedded in facade walls under internal retrofit conditions. The main objective is to identify the design variables that most strongly influence the linear thermal transmittance of these junctions and to quantify their relative importance.

Three specific objectives are addressed. First, the study evaluates how insulation continuity, insulation position relative to the column, insulation thickness, insulation thermal conductivity, and the presence of an air cavity affect thermal-bridge performance. Second, it analyzes how the position of the reinforced concrete column within the facade assembly influences linear thermal transmittance under different retrofit configurations. Third, it examines how improvements in wall thermal transmittance, when the column junction remains unresolved, modify the relative contribution of the thermal bridge to total envelope heat losses.

To address these objectives, the following research questions are examined:

RQ1. Which design variables most strongly influence the linear thermal transmittance of reinforced concrete columns embedded in facade walls under internal retrofit conditions?

RQ2. How do insulation continuity, insulation position relative to the column, insulation thickness, insulation thermal conductivity, the presence of an air cavity, and column position within the facade affect thermal-bridge performance?

RQ3. To what extent does improving wall thermal transmittance without resolving the column junction increase the relative contribution of the thermal bridge to total envelope heat losses?

By combining a Spanish retrofit context with a parametric and regression-based analysis, the study provides practical evidence for improving internal facade retrofit strategies and for reducing the energy penalty associated with structural thermal bridges in existing residential buildings.

The document is organized as follows. Section 2 presents a literature review. Section 3 describes the materials and methods, including the data sources and the generated database. Section 4 presents the results, and Section 5 discusses the findings and synthesizes the main conclusions.

2. Literature review

2.1 Thermal bridges and building energy performance

Thermal bridges have been widely recognized as critical weak points in the building envelope because they increase local heat transfer and may substantially affect the overall thermal performance of buildings. Earlier studies showed that simplified one-dimensional assessments may underestimate the effect of these non-uniformities and that two-dimensional modeling is often required to capture their influence on energy performance accurately. In residential buildings, thermal bridges may contribute significantly to transmission heat losses, especially when the overall thermal quality of the facade improves and the relative contribution of junctions becomes more pronounced [1-4].

The literature also shows that the magnitude of this effect depends not only on the geometry of the junction but also on the thermal properties and continuity of the envelope layers. In this regard, the correction of thermal bridges has been associated with lower heat losses and, in some cases, with favorable energy and cost implications, particularly in retrofit contexts. This is especially relevant in Mediterranean and warm climates, where the optimization of envelope details can improve building performance without necessarily requiring major structural interventions [3, 5].

2.2 Thermal-bridge studies on specific junctions

Previous research has addressed a variety of thermal-bridge junctions in building envelopes. Among the most frequently studied are balcony slabs, facade corners, slab edges, heads of openings, and window installation details. These studies consistently show that the thermal performance of the junction depends on the material configuration, the continuity of the insulation layer, and the constructive detailing adopted at the interface between building elements [4, 26-28].

More recent work has also examined design improvements for thermal bridges in residential facades under increasingly demanding energy-efficiency standards. For example, studies on double-brick facades and slab junctions have shown that the design of the envelope detail can have a strong influence on heat losses and on the feasibility of achieving high-performance building targets. Review-based studies have further confirmed that recurring thermal bridges in floors, slabs, and facade junctions remain one of the main technical barriers to improving envelope thermal continuity in both new construction and retrofit projects [13, 14, 29].

2.3 Internal retrofit and the persistence of structural thermal bridges

Although external insulation systems are widely considered one of the most effective solutions for reducing facade thermal bridges, they cannot always be applied in existing buildings. Legal, architectural, and technical constraints may limit the use of ETICS, making internal insulation a more viable retrofit strategy in some cases. However, internal retrofit often leaves structural thermal bridges unresolved, particularly where reinforced concrete elements are embedded in masonry facades. Under these conditions, the improvement of wall thermal transmittance may increase the relative importance of the remaining junction losses [2, 13, 14].

This issue is especially relevant in the Spanish residential stock, where facade systems based on brick masonry and reinforced concrete structural elements are common. In such buildings, columns integrated into facade walls may interrupt insulation continuity and generate thermal bridges that are difficult to correct when retrofit is performed from the interior side. Despite their practical importance, these column-induced thermal bridges have received less attention than other junctions such as balconies, slab edges, or openings. Studies addressing pillar–wall interactions in warm climates confirm their influence on energy demand, but the available evidence remains more limited than for other types of facade junctions [30].

2.4 Modeling approaches and identification of influential variables

Beyond the descriptive analysis of specific constructive details, some studies have focused on identifying the variables that most strongly affect thermal-bridge performance. Statistical modeling and sensitivity analysis have proven useful for this purpose because they allow the relative importance of geometry, material properties, and insulation strategies to be quantified. Larbi [31] showed that statistical modeling can provide a practical framework for estimating heat transfer in building thermal bridges, while Capozzoli, Gorrino and Corrado [32] demonstrated the usefulness of sensitivity analysis in identifying the parameters with the strongest influence on thermal-bridge behavior.

These approaches are particularly valuable in retrofit studies because they support design-oriented decision-making. Rather than evaluating a single construction detail in isolation, parametric and regression-based methods make it possible to compare a large number of alternatives and to determine which variables should be prioritized to reduce

heat losses. This is especially relevant when retrofit measures must be selected under practical constraints such as limited space, preservation requirements, or the impossibility of applying external insulation.

2.5 Research gap

Taken together, the existing literature confirms three points. First, thermal bridges can significantly affect the energy performance of building envelopes. Second, the effectiveness of mitigation measures depends strongly on the geometric and material configuration of the junction. Third, parametric and statistical approaches are useful for identifying the variables that govern thermal-bridge performance. However, less attention has been paid to reinforced concrete columns embedded in facade walls under internal retrofit conditions, despite their relevance in existing residential buildings where external insulation cannot be applied [14, 29-31].

Accordingly, further evidence is needed to determine which design variables most strongly influence the linear thermal transmittance of facade-integrated reinforced concrete columns and how these variables affect heat losses when retrofit is carried out from the interior. Addressing this gap is important not only for improving local constructive detailing, but also for reducing the energy penalty associated with unresolved structural thermal bridges in retrofitted residential facades.

3. Materials and methods

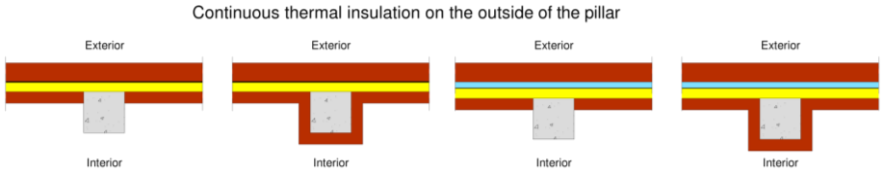
3.1 Data

3.1.1 Population and sample

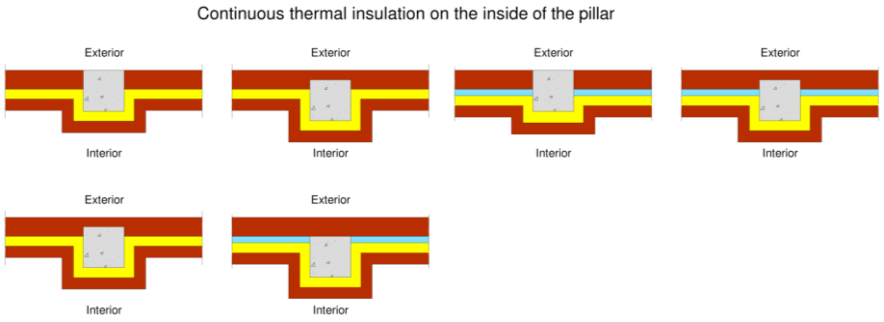
In Spain, DB-HE [9] classifies thermal bridges within the building envelope into five groups: a) integrated into the envelopes; b) at envelope junctions; and c) facade corners or junctions; d) junctions between cantilevered elements and facades; and e) junctions between interior partitions and the envelope. This study focuses on columns integrated into facades, corresponding to the first group.

To construct the dataset, two of the most common facade typologies in Spain were selected and analyzed: exposed brick facades and rendered brick facades with a single-layer mortar finish (Figure 5). Additionally, a column dimension of 0.25 × 0.25 m was established as a fixed parameter, and different construction solutions were developed based on combinations of the following conditions:

a) The classification of thermal bridges for columns integrated into envelopes provided by DA DB-HE/3 [8], which comprises 22 solutions based on the continuity and position of insulation relative to the column. These are distributed as follows: 4 solutions with continuous insulation placed on the exterior of the column (Group 1, Figure 3a), 6 solutions with continuous insulation placed on the interior of the column (Group 1, Figure 3b), and 12 solutions with discontinuous insulation (Group 2, Figure 4).



(a)



(b)

Figure 3. Group 1: Columns integrated into facades with continuous insulation. Author's own creation based on DA DB-HE/3 [8].

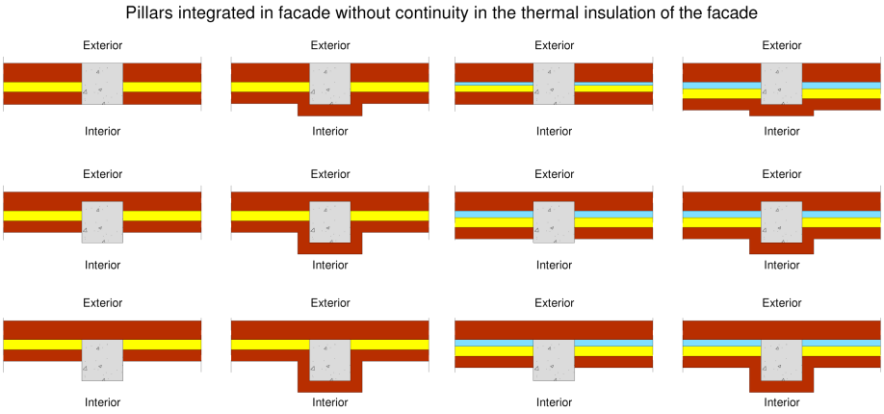


Figure 4. Group 2: Columns integrated into facades with discontinuous insulation. Author's own creation based on DA DB-HE/3 [8]

175

b) The relationship between the thickness of the thermal insulation surrounding the column and that of the facade, with possible values of 0.5, 1.0, and 1.5. When applied to the previous combinations, this results in 38 solutions per facade typology.

c) The thickness of the facade's thermal insulation, with possible values of 0.06, 0.08, 0.10, 0.12, and 0.14

180 m. Applying these values to the previous combinations yields 190 solutions per facade typology.

d) The thermal conductivity of the insulation, with possible values of 0.029, 0.032, 0.034, 0.036, and 0.040 W/m·K. When applied to the previous combinations, this results in 950 solutions per facade typology.

Therefore, a database comprising 950 solutions per facade typology was generated (Figure 5).

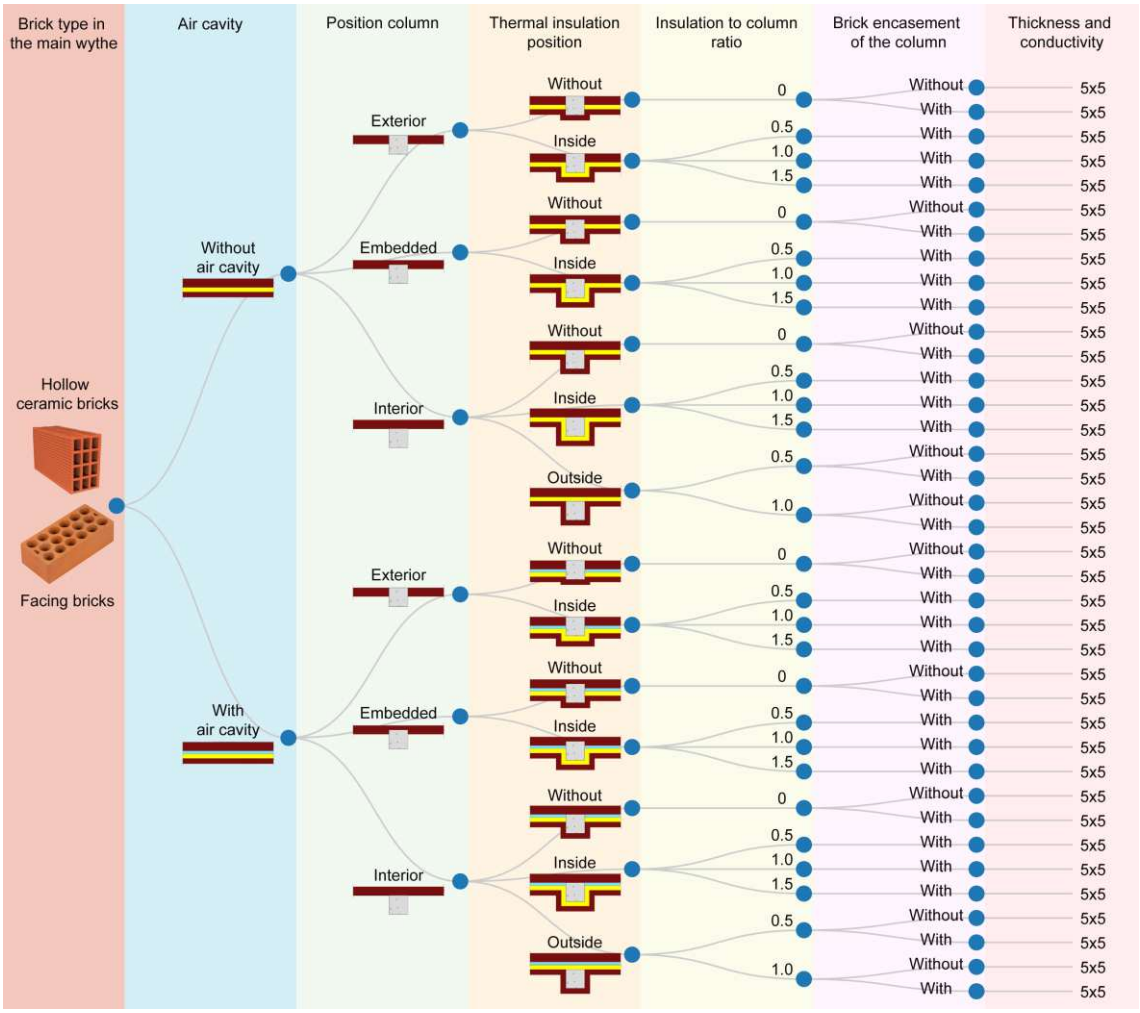
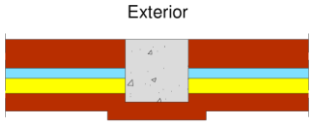
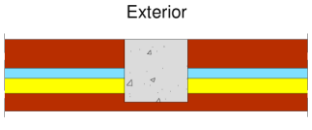
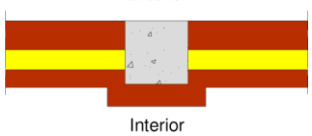
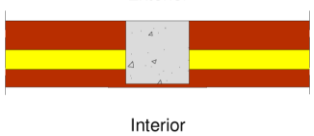
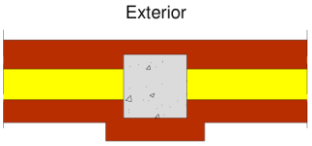
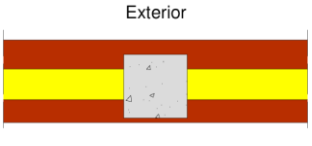
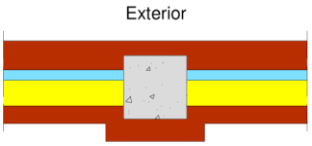
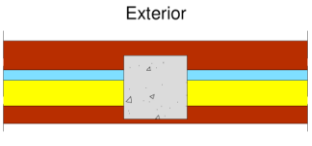


Figure 5. Diagram of the database solutions.

Once the 950 solutions per facade typology were graphically represented, it was observed that some solutions were thermally equivalent, repeating due to the combinations of different criteria. As a result, 95 solutions were discarded (Table 1). The final sample consisted of 855 solutions per facade typology, for a total of 1,710 solutions.

Table 1. Example of thermally equivalent solutions, showing the diagrams of the adopted solution (a) and the discarded solution (b).

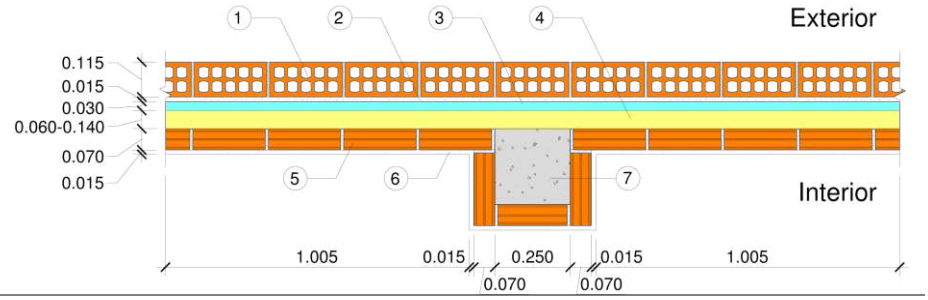
Similar solutions	
(a) Adopted solution	(b) Discarded solution
	
	

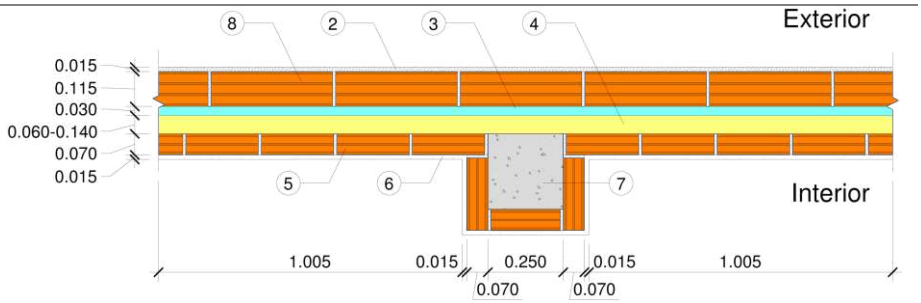
Similar solutions	
(a) Adopted solution	(b) Discarded solution
	
	

3.1.2 Numerical calculation of thermal transmittance

Table 2 presents the cross-sections of the facade typologies analyzed in this study, including the materials used and their respective thicknesses. Their thermal properties are also provided, based on the Catalog of Construction Elements (CEC) of the CTE [33], which references the thermal values established in the UNE-EN ISO 10456 [34]. The thermal resistance of the unventilated air cavity was obtained from DA DB-HE/1 [35].

Table 2. Materials used in the facade, showing thickness, thermal conductivity, and thermal resistance.

Id	Material	Thickness [m]	Thermal Conductivity (λ) [W/m·K].	Thermal Resistance (R) [m²·K/W]
1	1/2 metric or Catalan perforated brick (thickness 80–100 mm)	0.115	0.543	0.212
2	Cement or lime mortar for masonry and plastering (density 1000–1250 kg/m³)	0.015	0.550	0.027
3	Unventilated air cavity	0.030	0.173	0.173
4	Mineral wool (MW)	0.060, 0.080, 0.100, 0.120, 0.140	0.029, 0.032, 0.034, 0.036, 0.040	From 0.150 to 4.828
5	Double hollow brick partition [thickness 60–90 mm]	0.070	0.375	0.187
6	High-strength gypsum (density 900–1200 kg/m³)	0.015	0.430	0.035
7	Reinforced concrete (density 2300–2500 kg/m³)	0.250	2.300	0.109
8	Triple hollow brick partition [thickness 60–90 mm]	0.115	0.435	0.264
Facade typology	**Exposed brick**			

	Hollow brick facade with a single-layer mortar render	

The thermal transmittance of the facade (U_i) was determined using the following equation (1) [35]:

$$U_i = \frac{1}{(R_{si}+R_1+R_2+\ldots+R_n+R_{se})} \quad (1)$$

Where:

R_{si} internal surface resistance. According to [35] UNE-EN ISO 6946 [36], for horizontal heat flow, the value is 0.13 [m²·K/W].

R_{se} external surface resistance. According to [35] UNE-EN ISO 6946 [36], for horizontal heat flow, the value is 0.04 [m²·K/W].

$R_{1,2,..,n}$ thermal resistance of the different facade components [m²·K/W] calculated as $R_n=e/\lambda$, where e is the thickness of the layer [m] and λ is the design thermal conductivity of the material composing the layer [W/m·K].

3.1.3 Numerical calculation of thermal bridges

The thermal bridges were calculated using two-dimensional modeling, based on the thermal transmission equation by superposition of heat flows (2)) [8].

$$\Phi_{2D} = [\sum(U_i\, A_i) + \sum(\Psi_j\, L_j)] \cdot (\theta_i - \theta_e) \quad (2)$$

By rearranging Equation 2, the linear thermal transmittance, ΨL (3)), was obtained. This parameter represents the one-dimensional thermal transmittance occurring in the elements adjacent to the thermal bridge:

$$\Psi L = \frac{\Phi_{2D}}{(\theta_i - \theta_e)} - \sum U_i\, A_i \quad (3)$$

Where:

Ψ linear thermal transmittance [W/m·K]

Φ_{2D} heat flow through the analyzed element obtained by two-dimensional modeling [W]

L length of the junction [m]

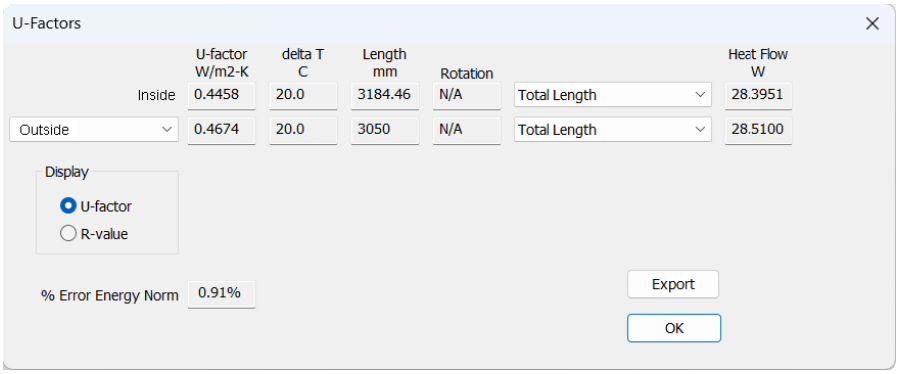
Θ_i- Θ_e temperature difference between interior and exterior. The temperature difference used in the calculation corresponds to winter conditions, with Θ_i = 20ºC and Θ_e = 0ºC [K] [8]

U_i thermal transmittance of the adjacent element i [W/m²·K]

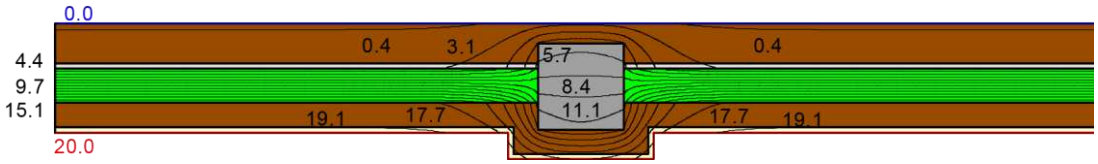
A_i surface area to which the Ui value applies [m²]

In this study, heat flow per linear meter (Φ_L) was calculated using the finite element software THERM version 7.8 [37]. First, the section was drawn in AutoCAD [38], and then imported into THERM. Once the detail was loaded, the materials composing the construction elements were defined, with thermal conductivity values obtained from the Catalog of Construction Elements of the CTE [33] and based on the material library developed by Campos Gordillo [39]. Subsequently, the boundary conditions were established, the maximum allowable error for the energy calculation was set, and the simulation was calculated.

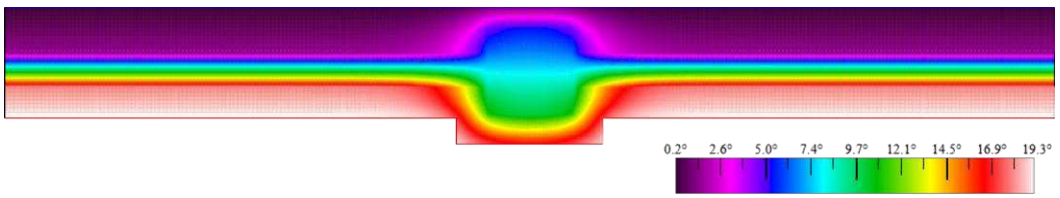
Once the calculation was completed, THERM displays a table with the heat flow (Φ_{2D}) for the interior and exterior dimensions (Figure 6a). In addition, isotherms showing the temperature distribution are automatically generated (Figure 6b). Among the different options for presenting results, THERM also allows visualization of a thermogram in a rainbow color scale of the analyzed construction element (Figure 6c), providing a graphical representation of the thermal bridge behavior.



a)



b)



c)

Figure 6. a) Table with the heat flow (Φ_{2D}) for the interior and exterior dimensions; b) Isotherms illustrating the temperature distribution; c) Thermogram of the analyzed thermal bridge.

3.1.4 Data description

Table 3 summarizes the 10 variables collected for this study, indicating which were included in the final regression model. The variables *U_wall, Heat_flow*, and *TB_energy_loss_pct* were not incorporated into the regression model because they exhibit collinearity with other variables already included. These three variables are derived from, or dependent on, characteristics of the envelope and the thermal bridge, which are already accounted for in the model

through more fundamental explanatory variables, such as insulation thickness and thermal conductivity, continuity of insulation, and the presence of an air cavity. Including them would create redundancy, artificially inflate the coefficients, and destabilize the estimation. Therefore, they were only used for exploratory analysis and graphical representation and were not included in the OLS or QR models.

Table 3. Variables included in the study.

Variable	Feature	Scale of measure	Description of the variables	Used in the model
Main wythe	*Main_wythe_PFB* *Main_wythe_THB*	dummy	Dummy variable indicating the type of Main wythe: PFB (perforated brick) or THB (triple hollow brick with plaster finish).	Yes
Column and main wythe	*Position_column_MS_exterior* *Position_column_MS_embedded* *Position_column_MS_interior*	dummy	Dummy variables indicating the position of the column relative to the main wythe of the envelope were defined. Three positions of the column relative to the main wythe: flush with exterior of the main wythe, embedded (1/3), and flush with interior.	Yes
Position of insulation relative to column	*Insulation_position_column_without* *Insulation_position_column_outside* *Insulation_position_column_insider*	dummy	Dummy variables indicating the position of the insulation relative to the column.	Yes
Brick encasement of the column	*Brick_encasement_column*	dummy	Dummy variable indicating whether the column is encased on the interior side with double hollow brick (DHB).	Yes
Air cavity	*Cavity_wall*	dummy	Dummy variable indicating whether the envelope wall includes an air cavity.	Yes
Insulation-to-column ratio	*Insulation-column ratio_0* *Insulation-column ratio_0.5* *Insulation-column ratio_1.0* *Insulation-column ratio_1.5*	dummy	Dummy variables indicating the relationship between the thickness of the insulation in the envelope wall and the column area. Ratios: 0, no insulation in column; 0.5, insulation thickness in the column is half of that in the envelope wall; 1, the insulation thickness in the column is equal to that in the envelope wall; 1.5, the insulation thickness in the column is 1.5 times that in the envelope wall.	Yes
Insulation thickness	*Insulation_thickness_cm*	numerical	Continuous variable indicating the thickness of the insulation in centimeters. Five values considered: 6, 8, 10, 12, 14 cm.	Yes
Insulation conductivity	*Insulation_conductivity_x1000*	numerical	Continuous variable indicating the thermal conductivity of the insulation placed in the envelope wall. Five conductivity values considered: 0.029, 0.032, 0.034, 0.036, 0.040 W/m·K. Continuous variable indicating the thermal conductivity of the insulation in the envelope wall, multiplied by 1000 to improve interpretability (e.g., for each 0.001 increase/decrease in conductivity).	Yes
Thermal transmittance	*U_wall*	numerical	Continuous variable indicating the thermal transmittance of the envelope wall in $W/m^2 \cdot K$. (Note: not included in the regression model due to collinearity, but used in scatter plots).	No
Heat flow	*Heat_flow*	numerical	Continuous variable indicating the heat flux (Φ) obtained in Therm, expressed in watts (W). (Note: not included in the regression model due to collinearity, but used in scatter plots).	No
Thermal bridge energy	*TB_energy_loss_pct*	numerical	Continuous variable indicating the percentage of energy lost through the thermal bridge.	No

Variable	Feature	Scale of measure	Description of the variables	Used in the model
			(Note: not included in the regression model due to collinearity, but used in scatter plots).	
Dependent variable	*Ψcolumn_int*	numerical	Continuous variable indicating the linear thermal transmittance of the thermal bridge, measured with interior dimensions, expressed in W/m·K.	Yes

The descriptive statistics of the variables used in this study are presented in Table 4.

Table 4. Descriptive statistics of the variables included in the study.

Coded variable	Continuous Variables				Dummy Variables		
	Mean	*SD*	Min.	Max.	Coding.	Freq.	Percent.
Main_wythe_THB	-	-	-	-	1	855	50.0%
Main_wythe_PFB	-	-	-	-	1	855	50.0%
Position_column_MS_interior	-	-	-	-	1	900	52.6%
Position_column_MS_exterior	-	-	-	-	1	350	20.5%
Position_column_MS_embedded	-	-	-	-	1	460	26.9%
Insulation_position_column_insider	-	-	-	-	1	900	52.6%
Insulation_position_column_outside	-	-	-	-	1	400	23.4%
Brick_encasement_column	-	-	-	-	1	1350	78.9%
Cavity_wall	-	-	-	-	1	840	49.1%
Insulation-column ratio_0	-	-	-	-	1	410	24.0%
Insulation-column ratio_0.5	-	-	-	-	1	500	29.2%
Insulation-column ratio_1.0	-	-	-	-	1	500	29.2%
Insulation-column ratio_1.5	-	-	-	-	1	300	17.5%
Insulation_thickness_cm	9.870	2.822	6.000	14.000	-	-	-
Insulation_conductivity_x1000	34.200	3.711	29.000	40.000	-	-	-
U_wall	0.291	0.074	0.176	0.469	-	-	-
Heat_flow	21.029	6.792	10.168	43.056	-	-	-
TB_energy_loss_pct	27.100	11.704	9.50	57.180	-	-	-
Ψcolumn_int	0.307	0.212	0.051	0.870	-	-	-

Notes: *N*=1710. *SD*: Standard deviation.

3.2 Statistical Modeling

To assess the impact of the thermal bridge generated by the columns integrated into the facade wall, an exploratory data analysis was first conducted using graphical representation tools. Two statistical models were then estimated using SPSS for Windows version 25 [40]. Subsequently, the most influential variables in predicting the linear thermal transmittance of the column were identified. To do so, global approaches were applied: (1) standardized beta coefficients from the OLS model and (2) permutation importance analysis.

Permutation importance was estimated using the ELI5 library in Python [41]. This strategy quantifies the importance of a feature by evaluating the change in the model when it is excluded, by employing error or performance metrics. One of its main advantages is that it is model-agnostic, meaning it can be applied to any algorithm regardless of its internal structure. Furthermore, the resulting metric is easily interpretable and allows for comparisons across different models. In this study, the Mean Absolute Error (MAE) was used, representing the increase in error that would occur if the corresponding feature were removed. Finally, the method is computationally more efficient than other strategies

(Johnson and Lebreton [42], Groemping [43]), as it does not require retraining multiple models with different feature combinations.

3.2.1 Exploratory data analysis

The main objective of this section was to provide a graphical overview of the dataset. Accordingly, an exploratory data analysis (EDA) was conducted, following the approach defined by Tukey [44]. Distribution and scatter plots were generated to characterize the thermal behavior of both the facade wall and the integrated columns.

3.2.2 Regression model by OLS

The regression model was estimated using ordinary least squares (OLS), as expressed by the following equation

$$\Psi_i = \beta_0 + \sum_{k=1}^{n} \beta_k X_{ik} + e_i \quad (4)$$

Ψ_i is the linear thermal transmittance of solution i.
β_0 is the intercept term of the regression model.
β_k is the coefficient associated with characteristic "k"
X_{ik} is the value of characteristic "k" for observation "i".
e_i is the error term for observation "i"

To estimate an OLS model, the data must satisfy the assumptions of linearity, independence, homoskedasticity, normality, and absence of multicollinearity. Therefore, after estimating the OLS model, several diagnostic tests were conducted. First, the bivariate correlation matrix and scatter plots were examined to assess linear relationships among the variables. Second, the Durbin–Watson statistic was used to test the independence of sample observations. Third, the Breusch–Pagan test and a residual scatter plot were employed to evaluate heteroskedasticity. Fourth, the Kolmogorov–Smirnov test and a frequency diagram were used to assess the normality of residuals. Finally, the possible presence of multicollinearity was examined by analyzing the variance inflation factor (VIF) for the variables included in the model.

3.2.3 Quantile regression

Authors such as Sirmans et al. (2005) and Chasco Yrigoyen and Sánchez Reyes (2012) have highlighted several advantages of the quantile regression model over the OLS model. Specifically, it facilitates the identification of how each characteristic affects different parts of the conditional distribution of the dependent variable. It also controls for non-linearity, asymmetries leading to non-normality, the presence of outliers, and heteroskedasticity.

Quantile Regression was formulated following the framework proposed by [45] and further developed by [46] (5).

$$Y_i = X_i \beta_\theta + u_{\theta i} \quad (5)$$

Where: Y_i is the dependent variable; X_i is the matrix of independent variables; β_θ is the vector of parameters to be estimated for the θ-th quantile; and $u_{\theta i}$ is the random disturbance corresponding to the θ-th quantile.

Following [45], let X_i: i=1,…, n denote a sequence of K-dimensional row vectors of a known design matrix and suppose Y_i: i=1,…, n is a random sample on the regression process $u_i = Y_i X_i \beta$ having distribution function F. In this regression model, θ-th quantiles for the dependent variable are defined, conditional on the series X_i as Quant($Y_i|X_i$)=$X_i\beta_\theta$, with the only imposed condition being Quant ($u_{\theta i}|X_i$)=0. The θ-th regression quantile, with 0<θ<1, is then defined as any solution to the minimization problem:

$$\min_{\beta \in R^k} \left\{ \sum_{i \in \{i: Y_i \geq X_i \beta\}} \theta |Y_i - X_i \beta_\theta| + \sum_{i \in \{i: Y_i < X_i \beta\}} (1-\theta) |Y_i - X_i \beta_\theta| \right\} \quad (6)$$

Quantile regression is a nonlinear estimation method, solved using a linear programming model based on the simple algorithm. In this method, the absolute deviations are minimized with asymmetric weights [47]. In contrast, OLS minimizes the sum of squared residuals. Median regression is a special case of quantile regression corresponding to θ=0.5. It is the only case in which the weights are symmetric.

The goodness of fit of the quantile models was assessed using the *pseudo*-R1 statistic, based on absolute deviations [48]. This metric is useful for comparing different quantile models, but it is not directly comparable to the coefficient of determination obtained from OLS, which is based on the variance of the squared deviations. *Pseudo*-R1 is calculated as 1 minus the ratio between the sum of absolute deviations in the fully parameterized models and the sum of absolute deviations in the null (non-conditional) quantile model.

4. Results

4.1 Exploratory data analysis.

Distribution plots (Figure 7) were used to examine the thermal bridge behavior of reinforced concrete columns integrated into the facade envelope, considering two key factors: (1) the position of the thermal insulation relative to the column (none, behind, or in front of the column), and (2) the position of the column relative to the Main wythe of the envelope (aligned with the exterior, embedded within the envelope, or aligned with the interior). The analysis also distinguished between different combinations of insulation thickness and thermal conductivity. The results indicate that, when insulation is applied directly to the column (either on the interior or exterior side), the linear thermal transmittance of the thermal bridge is reduced by 65–75% compared to solutions without column insulation. The lowest thermal transmittance values occur when the insulation is continuous and located on the exterior side of the column.

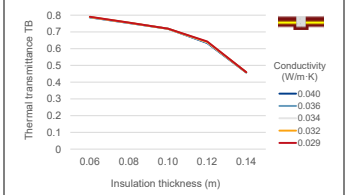
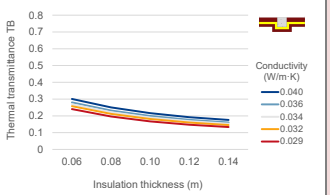
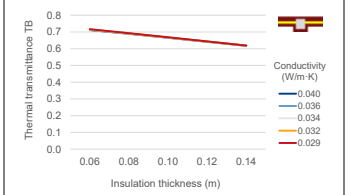
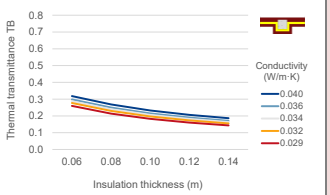
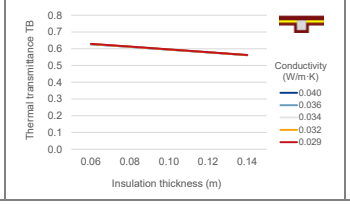
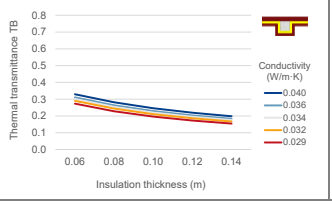
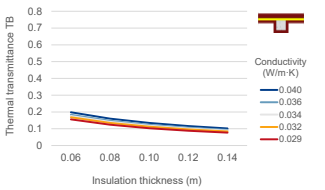
		Thermal insulation position on the column		
		No insulation in column	**Behind the column**	**In front of the column**
Column position relative to the Main wythe	**Exterior**			Solution not analyzed in this study
	Embedded			Solution not analyzed in this study
	Interior			

Figure 7. Linear thermal transmittances of thermal bridges as a function of column and insulation positions.
Note: Average values for LHT and LCV facade types. Solutions without air cavity, with brick encasement of the column, and with a 1 ratio between the column and envelope insulation are shown.

Figure 8 presents a scatter plot relating the thermal transmittance of the facade wall (*U_wall*) to the linear thermal transmittance of the column thermal bridge (*Ψcolumn_int*), with each point indicating the insulation thickness and thermal conductivity of the solution. The results reveal two distinct clusters: the first cluster corresponds to solutions without continuous insulation on the column, exhibiting higher linear thermal transmittance values; the second cluster corresponds to solutions with continuous insulation, showing significantly lower values. In both clusters, an upward trend is observed, indicating that as the thermal transmittance of the facade wall increases, the linear transmittance of the thermal bridge also increases.

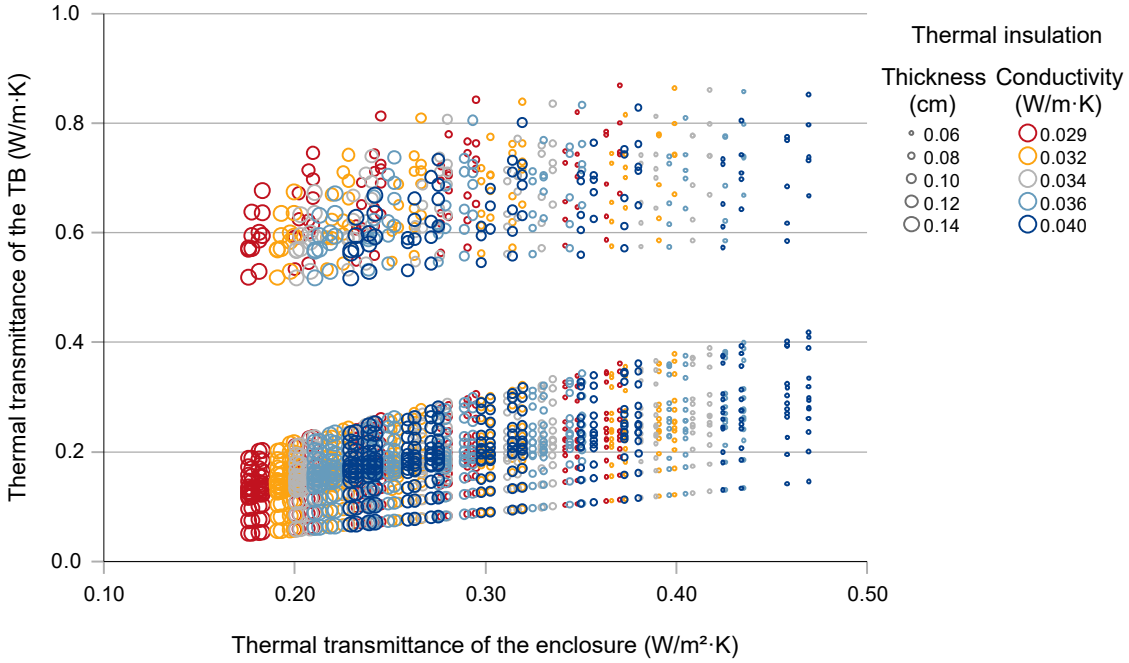


Figure 8. Scatter plot of the thermal transmittance of the facade wall and the linear thermal transmittance of the thermal bridge.

Figure 9 presents a scatter plot of the relationship between the thermal transmittance of the facade wall (U_wall) and the percentage of energy lost through the column thermal bridge. Two distinct groups of results are visible depending on the continuity of insulation in the column. Solutions without continuous insulation (upper group) show a steeper slope, indicating a larger relative contribution of the thermal bridge to the total energy losses of the envelope. This highlights the importance of insulation continuity at the column junction, revealing that in well-insulated facades (0.2 W/m²·K), the absence of column insulation results in approximately 60% of the energy losses occurring at the thermal bridge. In poorly insulated facades (0.5 W/m²·K), this percentage is reduced to around 30%, as losses are more evenly distributed across the envelope.

This finding underscores that, as the thermal performance requirements of the envelope increase, greater attention must be paid to resolving thermal bridges, due to the significant rise in their thermal transmittance and the resulting negative effect on the overall insulation performance of the system.

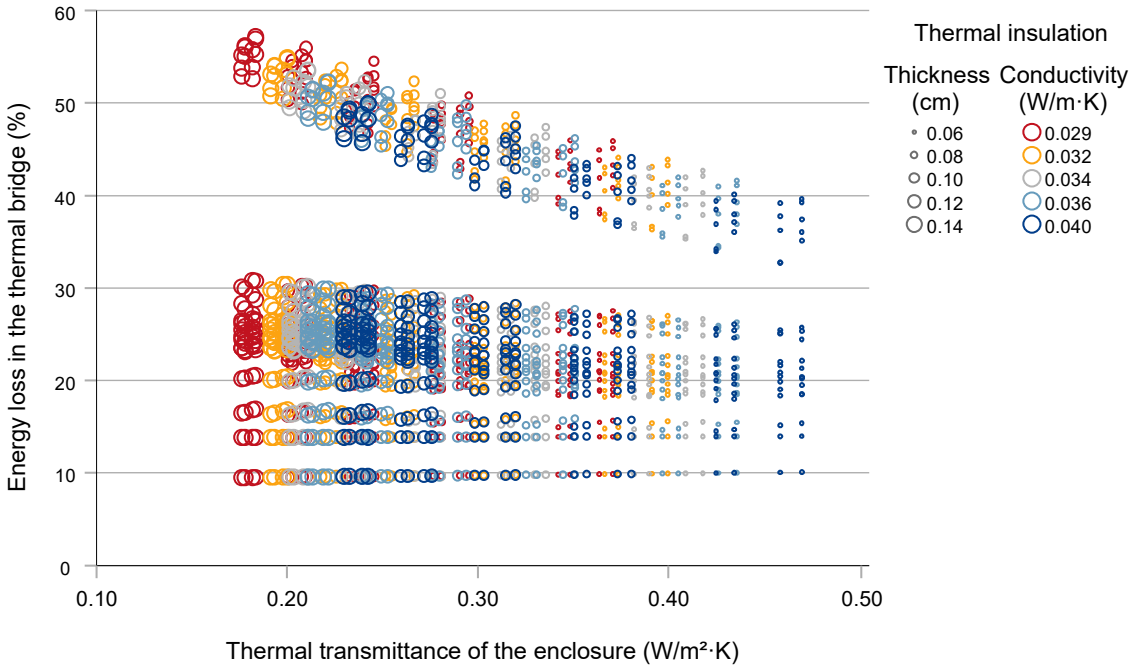


Figure 9. Scatter plot of the thermal transmittance of the facade wall and the percentage of energy losses through the column thermal bridge.

4.2 Regression model (OLS)

After estimating the OLS model, the assumptions of linearity, independence of errors, homoskedasticity, normality, and non-collinearity were evaluated. Linearity was assessed using partial plots of each independent variable against the dependent variable. The independence of sample observations was examined using the Durbin–Watson statistic, which yielded a value close to 2 [49, 50]. Heteroskedasticity was tested using the Breusch–Pagan test [51], which rejected the null hypothesis of homoskedasticity, indicating heteroskedasticity in the residuals (BP=492.87, df=11, p< 0.001). The normality of residuals was assessed using the Lilliefors (Kolmogorov–Smirnov) normality test, which also rejected the null hypothesis of normality (D=0.0423, p<0.001). Multicollinearity was evaluated using the Variance Inflation Factor (VIF). Past studies have suggested that multicollinearity may be problematic if the VIF values exceed 10 [52, 53]. In this case, most values were close to 1 (Table A1), with a maximum of 2.13, indicating no evidence of severe multicollinearity among the variables.

Table 5 presents the results of the OLS and QR regression model estimations. The OLS regression model achieved an adjusted coefficient of determination (R^2) of 0.973, indicating high explanatory power. For the QR models, the pseudo-R1 ranged from 0.793 to 0.891, suggesting a satisfactory fit to the data across quantiles. In addition, the mean absolute error (MAE), the mean square error (MSE), and the root mean squared error (RMSE) were calculated to assess model error.

Table 5. Results of the OLS and quantile regression (QR) models.

Characteristics	**OLS model**	**QR 10**	**QR 30**	**QR 50**	**QR 70**	**QR 90**
(Intercept)	0.694 *** (0.009)	0.535 *** (0.004)	0.604 *** (0.004)	0.645 *** (0.005)	0.712 *** (0.007)	0.768 *** (0.011)
Main_wythe_PFB	0.015 *** (0.002)	0.000 (0.001)	0.002 ** (0.001)	0.004 *** (0.001)	0.004 ** (0.001)	0.007 ** (0.002)
Main_wythe_THB (ref)	-	-	-	-	-	-
Position_column_MS_exterior	0.002 (0.002)	-0.027 *** (0.001)	-0.025 *** (0.001)	-0.021 *** (0.001)	-0.017 *** (0.002)	-0.016 *** (0.003)

Characteristics	OLS model	QR 10	QR 30	QR 50	QR 70	QR 90
Position_column_MS_embedded	0.018 *** (0.002)	-0.011 *** (0.001)	-0.009 *** (0.001)	-0.007 *** (0.001)	-0.006 ** (0.002)	0.001 (0.003)
Position_column_MS_interior (ref)						
Insulation_position_column_outside	-0.102 *** (0.003)	-0.102 *** (0.001)	-0.097 *** (0.001)	-0.099 *** (0.002)	-0.104 *** (0.002)	-0.106 *** (0.004)
Insulation_position_column_insider (ref)	-	-	-	-	-	-
Brick_encasement_column	-0.008 *** (0.002)	0.032 *** (0.001)	0.029 *** (0.001)	0.022 *** (0.001)	0.010 *** (0.002)	0.001 (0.003)
Cavity_wall	-0.020 *** (0.002)	-0.012 *** (0.001)	-0.013 *** (0.001)	-0.014 *** (0.001)	-0.015 *** (0.001)	-0.016 *** (0.002)
Insulation-column ratio_0 (ref)	-	-	-	-	-	-
Insulation-column ratio_0.5	-0.382 *** (0.003)	-0.312 *** (0.001)	-0.362 *** (0.001)	-0.390 *** (0.002)	-0.423 *** (0.002)	-0.441 *** (0.003)
Insulation-column ratio_1.0	-0.442 *** (0.003)	-0.364 *** (0.001)	-0.418 *** (0.001)	-0.446 *** (0.002)	-0.482 *** (0.002)	-0.508 *** (0.003)
Insulation-column ratio_1.5	-0.465 *** (0.003)	-0.385 *** (0.001)	-0.438 *** (0.001)	-0.469 *** (0.002)	-0.505 *** (0.002)	-0.532 *** (0.004)
Insulation_thickness_cm	-0.014 *** (0.000)	-0.013 *** (0.000)	-0.013 *** (0.000)	-0.013 *** (0.000)	-0.014 *** (0.000)	-0.014 *** (0.000)
Insulation_conductivity_x1000	0.003 *** (0.000)	0.004 *** (0.000)	0.004 *** (0.000)	0.004 *** (0.000)	0.004 *** (0.000)	0.003 *** (0.000)
Statistics						
Adj. R^2	0.973	-	-	-	-	-
Pseudo-R1	-	0.793	0.826	0.851	0.884	0.881
MAE	0.026	0.037	0.025	0.023	0.026	0.041
MSE	0.001	0.004	0.002	0.001	0.002	0.003
RMSE	0.034	0.065	0.045	0.038	0.042	0.059

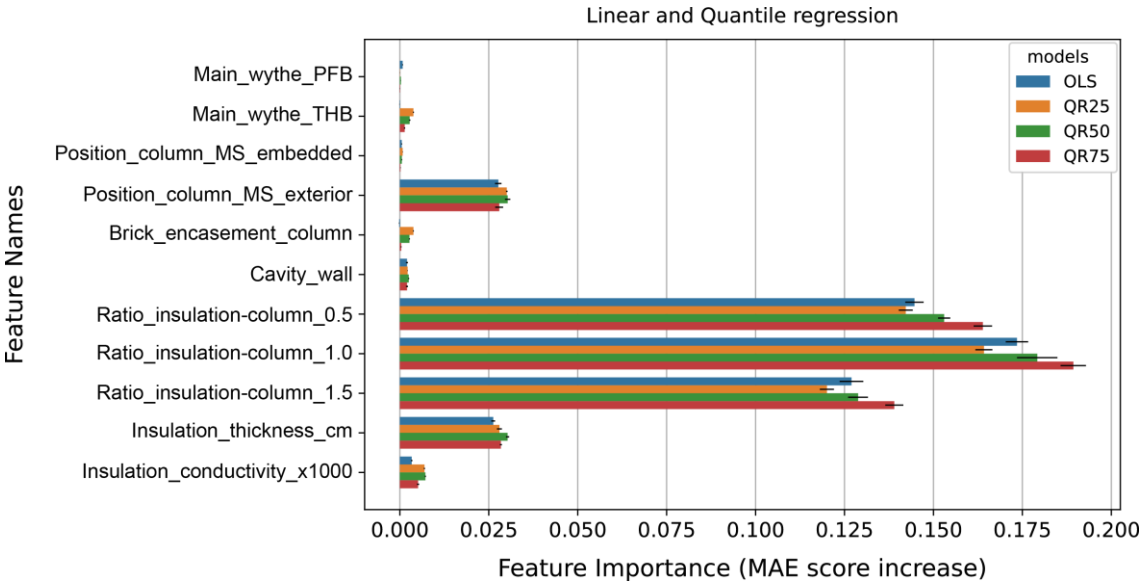
Notes: dependent variable Ψ_{column_int}; $N = 1710$; *** p < 0.001, ** p < 0.01, * p < 0.05. R^2 denotes the coefficient of determination. MAE, MSE, and RMSE denote the mean absolute error, mean square error, and root mean squared error, respectively. The pseudo-R1 measure is reported following [48].

Since the OLS model is estimated in levels, the estimated coefficients can be interpreted as absolute changes in the linear thermal transmittance of the thermal bridge, expressed in W/m·K. The results indicate that using facing brick in the Main wythe increases the linear thermal transmittance of the column by 0.015 W/m·K compared with triple hollow brick. Regarding the position of the column relative to the envelope, and taking the column aligned with the interior as the reference category, the linear thermal transmittance increases by 0.002 W/m·K when the column is aligned with the exterior and by 0.018 W/m·K when it is embedded. Conversely, when thermal insulation is continuous on the exterior side of the column, the linear thermal transmittance decreases by 0.102 W/m·K compared with the case with continuous insulation on the interior side. Similarly, the presence of an air cavity in the envelope and the interior encasement of the column reduce the linear thermal transmittance by 0.020 W/m·K and 0.008 W/m·K, respectively.

The results indicate that the greatest reduction in the linear thermal transmittance of the column occurs when continuity of the thermal insulation in the column is ensured. Depending on the ratio between the thickness of the column insulation and that of the envelope, reductions of 0.382 W/m·K, 0.442 W/m·K, and 0.465 W/m·K are obtained for ratios of 0.5, 1.0, and 1.5, respectively. To identify the most influential variables in predicting the linear thermal transmittance of the thermal bridge, two complementary analyses were conducted. The first involved examining the standardized beta coefficients of the OLS model. (Table A1). The results show that the most effective strategies for reducing linear thermal transmittance in column thermal bridges are: (a) ensuring continuity of thermal insulation in the column (*Insulation-column ratio_0.5*, *Insulation-column ratio_1.0*, *Insulation-column ratio_1.5*); (b) placing the insulation on the exterior side of the column (*Insulation_position_column_outside*); and (c) increasing the thickness of the thermal insulation in both the envelope and the column (*Insulation_thickness_cm*). Less influential factors include reducing the thermal conductivity of the insulation (*Insulation_conductivity_x1000*) and incorporating an air cavity of

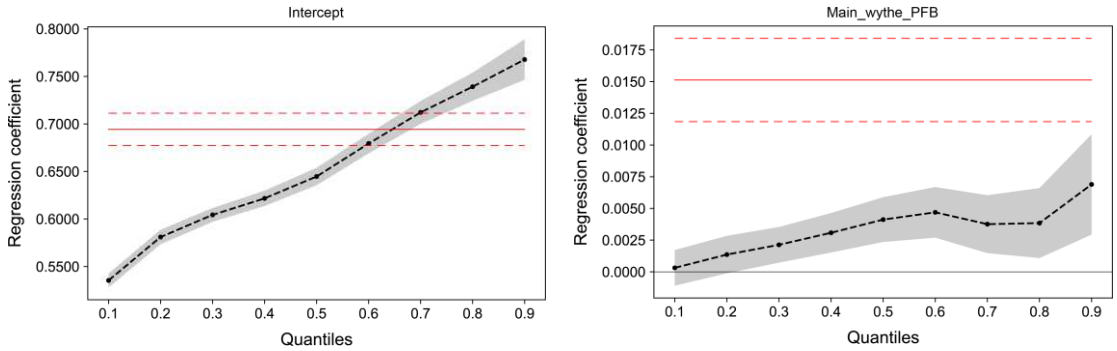
385 at least 3 cm in the envelope (*Cavity_wall*). Finally, the variables with the least impact are the type of brick used in the construction of the Main wythe (triple hollow brick or facing brick), the position of the column relative to the Main wythe (interior, embedded, or exterior), and the interior encasement of the column (*Brick_encasement_column*).

The second analysis consisted of a more detailed assessment of variable importance using a permutation approach based on the increase in Mean Absolute Error (MAE). The results are presented in Figure 10. This analysis confirms 390 the findings obtained from the standardized coefficients, again highlighting that continuity of insulation in the column is the most influential variable. Moreover, the quantile analysis (25th, 50th, and 75th) indicates that the importance of this variable is greater in the upper quantiles of the distribution, which correspond to less thermally efficient solutions. The remaining variables exhibit similar behavior in both the QR and OLS model estimations.

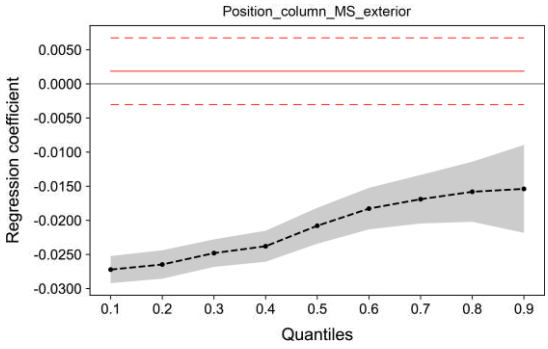


395 Figure 10. Relative importance of the variables based on MAE for the OLS and QR models.

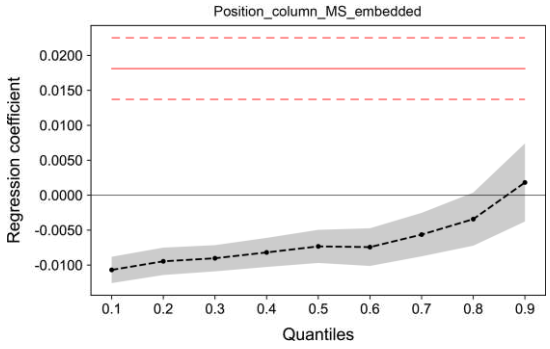
Figure 11 presents the graphical representation of the quantile regression results, illustrating how the slope of each regression coefficient varies across different quantiles of the dependent variable. The horizontal axis shows the quantiles while the vertical axis represents the estimated regression coefficients. The dotted line with markers represents 400 the quantile regression estimates across quantiles, with the shaded blue area indicating their 95% confidence intervals. The OLS regression coefficient is shown as a solid red horizontal line, with its 95% confidence interval represented by red dashed lines. If the confidence intervals of either the OLS or QR estimates include zero, the corresponding coefficient is not statistically significant at the 95% confidence level. Furthermore, overlap between the confidence intervals of the QR and OLS estimates indicates that the coefficients at those quantiles are not statistically different 405 from the OLS estimate.



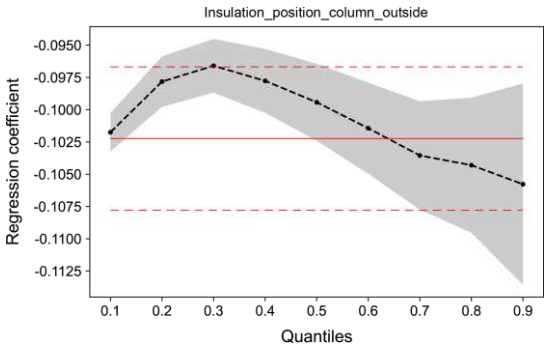
a) b)


Position_column_MS_exterior
Regression coefficient
0.0050
0.0000
-0.0050
-0.0100
-0.0150
-0.0200
-0.0250
-0.0300
0.1 0.2 0.3 0.4 0.5 0.6 0.7 0.8 0.9
Quantiles

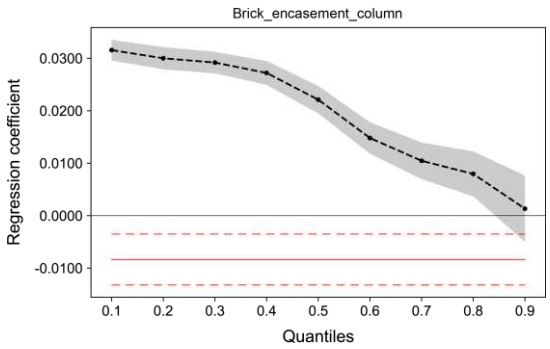
c)


Position_column_MS_embedded
Regression coefficient
0.0200
0.0150
0.0100
0.0050
0.0000
-0.0050
-0.0100
0.1 0.2 0.3 0.4 0.5 0.6 0.7 0.8 0.9
Quantiles

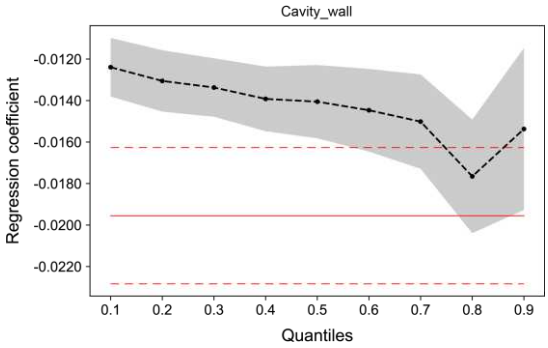
d)


Insulation_position_column_outside
Regression coefficient
-0.0950
-0.0975
-0.1000
-0.1025
-0.1050
-0.1075
-0.1100
-0.1125
0.1 0.2 0.3 0.4 0.5 0.6 0.7 0.8 0.9
Quantiles

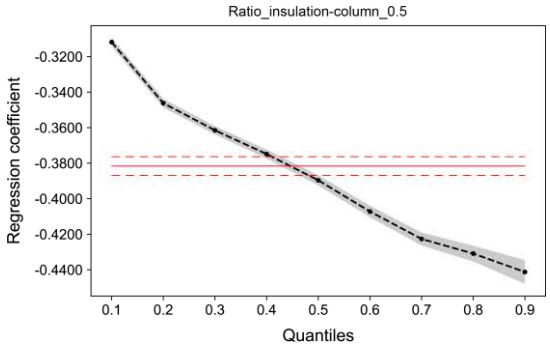
e)


Brick_encasement_column
Regression coefficient
0.0300
0.0200
0.0100
0.0000
-0.0100
0.1 0.2 0.3 0.4 0.5 0.6 0.7 0.8 0.9
Quantiles

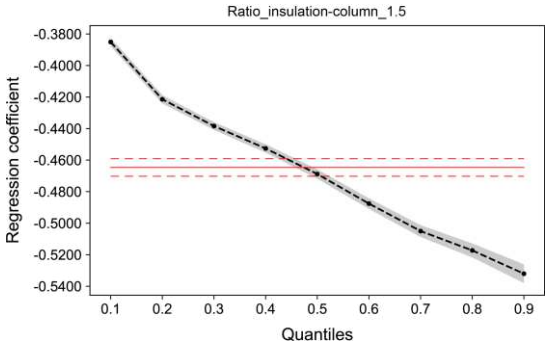
f)


Cavity_wall
Regression coefficient
-0.0120
-0.0140
-0.0160
-0.0180
-0.0200
-0.0220
0.1 0.2 0.3 0.4 0.5 0.6 0.7 0.8 0.9
Quantiles

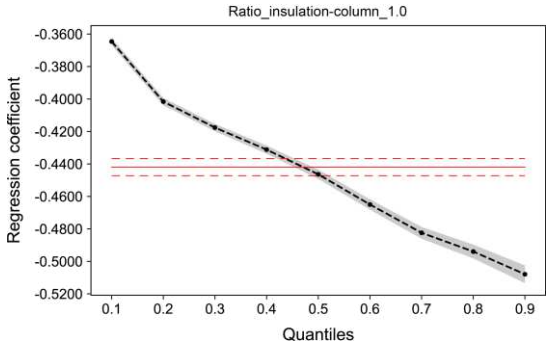
g)


Ratio_insulation-column_0.5
Regression coefficient
-0.3200
-0.3400
-0.3600
-0.3800
-0.4000
-0.4200
-0.4400
0.1 0.2 0.3 0.4 0.5 0.6 0.7 0.8 0.9
Quantiles

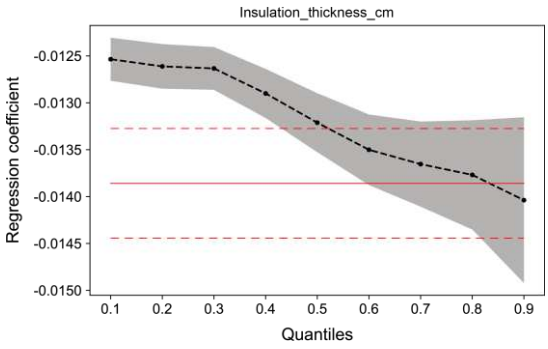
h)

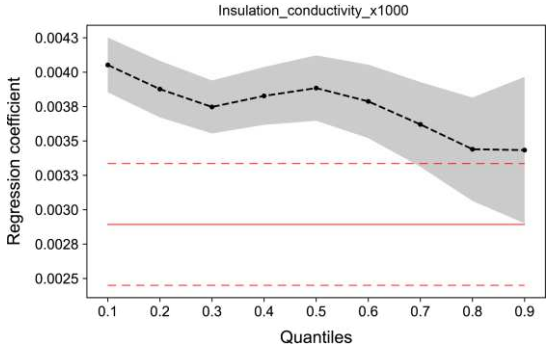

Ratio_insulation-column_1.5
Regression coefficient
-0.3800
-0.4000
-0.4200
-0.4400
-0.4600
-0.4800
-0.5000
-0.5200
-0.5400
0.1 0.2 0.3 0.4 0.5 0.6 0.7 0.8 0.9
Quantiles

i)


Ratio_insulation-column_1.0
Regression coefficient
-0.3600
-0.3800
-0.4000
-0.4200
-0.4400
-0.4600
-0.4800
-0.5000
-0.5200
0.1 0.2 0.3 0.4 0.5 0.6 0.7 0.8 0.9
Quantiles

j)


Insulation_thickness_cm
Regression coefficient
-0.0125
-0.0130
-0.0135
-0.0140
-0.0145
-0.0150
0.1 0.2 0.3 0.4 0.5 0.6 0.7 0.8 0.9
Quantiles


Insulation_conductivity_x1000
Regression coefficient
0.0043
0.0040
0.0038
0.0035
0.0033
0.0030
0.0028
0.0025
0.1 0.2 0.3 0.4 0.5 0.6 0.7 0.8 0.9
Quantiles

k) l)

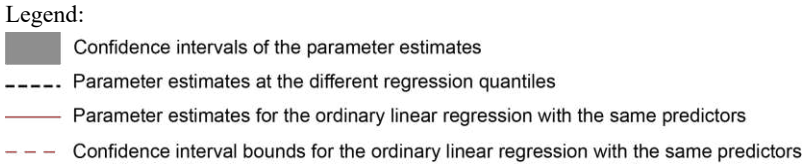
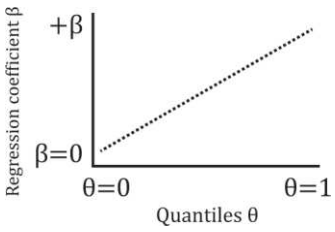
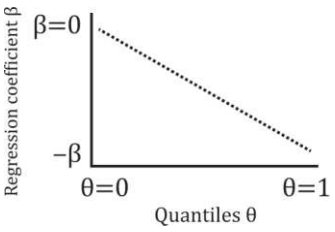
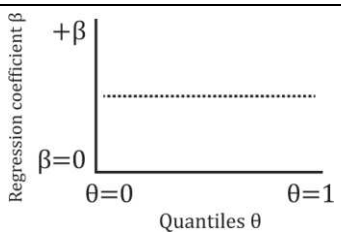
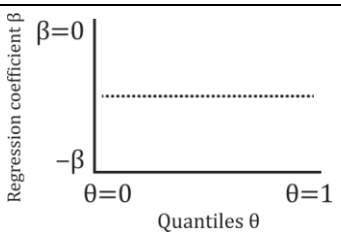
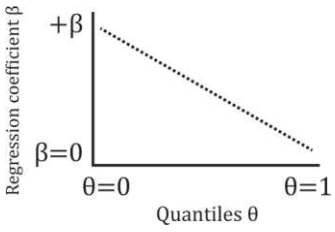
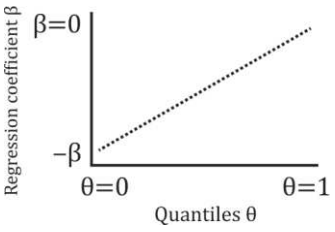


Figure 11. Graphical representation of regression by quantiles.

Table 6 provides a schematic interpretation of the quantile regression plots. For positive regression coefficients (+β), an upward trend indicates that the regression coefficient increases with higher quantiles. In this study, higher quantiles of the dependent variable correspond to solutions with greater linear thermal transmittance (higher energy losses, and thus less efficient solutions), whereas lower quantiles correspond to solutions with lower thermal transmittance (lower energy losses and more efficient solutions).

Table 6. Interpretation of the quantile regression plots.

Interpretation	Positive coefficients	Negative coefficients
The regression coefficient rises as the linear thermal transmittance of the thermal bridge increases.		
	(a)	(d)
The regression coefficient remains constant as the linear thermal transmittance of the thermal bridge increases.		
	(b)	(e)
The regression coefficient decreases as the linear thermal transmittance of the thermal bridge increases.		
	(c)	(f)

The graphical representation of quantile regression (Figure 11) shows that, for most variables, the estimated effects are more pronounced in the upper quantiles of linear thermal transmittance, indicating that the analyzed improvement strategies are particularly relevant for solutions with poorer thermal performance.

As shown in Figure 11, the intercept values for each quantile exhibit an upward trend, remaining positive and statistically significant across all quantiles. As the quantile increases, both the intercept value and the width of the confidence interval increase. This pattern is consistent with the data, as higher quantiles (representing less energy-efficient solutions) are associated with greater energy losses and higher variability in the estimates.

When analyzing the type of main facade layer (Figure 11b), the quantile regression model shows that solutions with facing brick (*Main_wythe_PFB*), compared to the reference layer (*Main_wythe_THB*), exhibit positive coefficients with higher quantiles. The QR coefficients differ statistically from the OLS estimate, indicating an increase of 0.015 W/m·K in the linear thermal transmittance of the thermal bridge when using facing brick instead of triple hollow brick. In the QR model, coefficients become statistically significant from the 30th quantile (QR30) onward, with values ranging from 0.002 and 0.007 W/m·K. This is considerably lower than the OLS estimate. This result indicates that using facing brick generates greater energy losses in less efficient thermal bridges (upper quantiles) as compared to more efficient ones (lower quantiles).

Regarding the position of the column relative to the Main wythe, taking the column aligned with the interior of the Main wythe (*Position_column_MS_interior*) as the reference, both the exterior-aligned column (Figure 11c) (*Position_column_MS_exterior*) and the embedded column (Figure 11d) (*Position_column_MS_embedded*) exhibit negative coefficients that increase as the quantile rises. In both cases, the results obtained differ from the OLS estimation, which yielded positive values that were not statistically significant for exterior-aligned column. The QR coefficients indicate that both solutions behave similarly up to the 60th quantile (0.6). Beyond this quantile, the slopes diverge: the embedded column shows pronounced upward increase, whereas the exterior-aligned column levels off. In other words, for embedded columns with less efficient thermal bridges (upper quantiles), the beta coefficient values increase more sharply than for columns aligned with the exterior.

With respect to the position of the insulation relative to the column, taking interior insulation (*Insulation_position_column_insider*) as the reference, the OLS and QR estimations yield similar results for insulation placed on the exterior side of the column (Figure 11e) (*Insulation_position_column_outside*). A turning point can be observed around the 30th quantile (0.3), indicating a change in trend. Up to this quantile, the beta coefficient values decrease, whereas beyond it they increase, reaching a maximum at the 90th quantile (0.9). This suggests that for higher quantiles (less efficient solutions), placing insulation on the exterior increases the magnitude of the negative beta coefficient, thereby reducing the linear thermal transmittance and improving the efficiency of the column compared to the solution with interior insulation.

Regarding the brick encasement of the column (*Brick_encasement_column*), the OLS and QR estimations differ in both magnitude and sign. As shown in Figure 11f, the variable exhibits a negative trend as the quantiles increase (less efficient solutions). Up to the 40th quantile (0.4), its impact on the thermal bridge remains nearly constant, around 0.03. Beyond this quantile, the effect diminishes, becoming practically negligible at the 90th quantile (0.9). These results indicate that brick encasement provides only a moderate improvement in more efficient solutions (lower quantiles) and does not significantly reduce the linear thermal transmittance in less efficient solutions (upper quantiles). Therefore, brick encasement cannot be considered an effective strategy for improving thermal bridges in less efficient solutions.

The next variable analyzed is the presence of an air cavity (Figure 11g) (*Cavity_wall*). Up to the 50th quantile (0.5), the results from the OLS and the QR estimations differ. However, beyond this quantile, both estimations show similar trends. The beta coefficients exhibit a negative increase as the quantiles rise, indicating that the inclusion of an air cavity reduces the linear thermal transmittance of the thermal bridge. This effect is more pronounced in the upper quantiles, which correspond to less efficient solutions.

Regarding the relationship between the thickness of the envelope insulation and that of the column, the reference variable was the absence of insulation in the thermal bridge (*Insulation-column ratio_0*). The results for the three scenarios considered (Figure 11h, i, j) (*Insulation-column ratio_0.5*, *10*, *15*) show a growing effect on reducing linear thermal transmittance, but with diminishing returns. That is, adding more insulation progressively yields smaller improvements. As observed, the coefficient reaches its highest (negative) value in the upper quantiles (i.e., less efficient solutions), revealing that covering the thermal bridge with insulation has a direct effect on reducing thermal transmittance. The magnitude of this effect diminishes as the insulation ratio in the column increases. At quantile 0.9,

increasing the ratio from 0.5 to 1 (*Insulation-column ratio_0.5, 10*) produces an absolute increase in the beta coefficient of 0.067 (0.508–0.441). However, increasing the ratio from 1 to 1.5 (*Insulation-column ratio_1.0, 15*), the same increment as before, results in an absolute increase of only 0.024 (0.532–0.508), 2.6 times smaller. This finding highlights the diminishing returns of improvements applied to the thermal bridge, indicating that even if the insulation ratio in the column is increased indefinitely, the resulting improvement in thermal transmittance would be minimal.

With respect to the thickness of thermal insulation (Figure 11k), the estimates from the OLS and QR models differ in magnitude up to quantile 0.6. Beyond this quantile, the estimates converge. The negative sign of the parameter indicates that increasing insulation thickness reduces the linear thermal transmittance of the thermal bridge. This reduction is more pronounced in the upper quantiles, which correspond to less efficient solutions.

Finally, regarding the thermal conductivity of the insulation (Figure 11l), the estimates differ in magnitude but share the same sign. The results indicate that thermal transmittance increases as the thermal conductivity of the insulation rises. This finding is consistent with expectations, since higher thermal conductivity reduces the insulating capacity of the material and thereby increases thermal transmittance. The quantile regression further shows that this effect is more pronounced in the upper quantiles, which correspond to less efficient solutions.

5. Discussion

The statistical analysis provides valuable insight into the behavior of the thermal bridge generated by reinforced concrete columns integrated into facades. In this respect, the study addresses RQ1 and shows that the construction variables do not contribute equally to the reduction of linear thermal transmittance. The results indicate that insulation continuity around the column is the factor that most strongly reduces the thermal penalty associated with this type of bridge, which confirms the importance of maintaining an uninterrupted thermal path across the structural element. This interpretation is consistent with previous studies showing that the effectiveness of thermal-bridge mitigation depends strongly on the continuity of the envelope layers and on the constructive definition of the junction [31, 32].

The results also provide useful criteria for optimizing facade design according to typology and for guiding the proper placement of constructive elements with the aim of minimizing heat losses. In particular, the study addresses RQ2 and shows that the position of the insulation relative to the column plays a decisive role in the thermal behavior of the junction. Among the analyzed solutions, those with continuous insulation placed on the exterior side of the column provide better thermal performance than those with insulation placed on the interior side. This result is physically coherent and agrees with previous studies on facade junctions and other non-uniform envelope details, where insulation placement and continuity are identified as key factors in reducing heat transfer [26, 27, 29].

At the same time, the results show that increasing insulation thickness reduces linear thermal transmittance, although the reduction becomes progressively smaller as thickness increases. This means that the improvement is not proportional and that, beyond a certain point, additional thickness provides diminishing returns. This issue is especially relevant in internal retrofit interventions, where thermal improvement must be balanced against space limitations, construction feasibility, and cost. In this regard, the results suggest that ensuring insulation continuity and optimizing its position relative to the column may be more effective than simply increasing thickness.

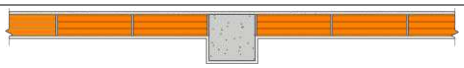
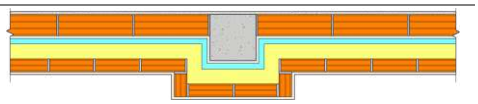
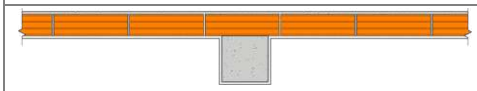
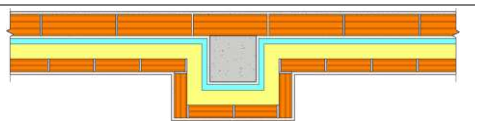
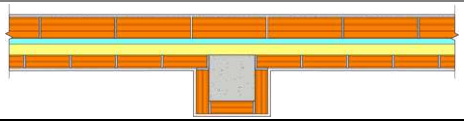
Other variables, such as insulation thermal conductivity and the presence of an air cavity, also influence the behavior of the thermal bridge, but their effect is secondary compared with continuity, insulation position, and thickness. This order of importance provides an objective basis for decision-making in retrofit interventions, because it helps identify which parameters should be prioritized when the intervention capacity is limited. In this sense, the combination of OLS and Quantile Regression is useful not only because it estimates average effects, but also because it shows how the influence of the variables changes across solutions with different levels of thermal performance. This interpretation is

in line with earlier studies that use statistical and sensitivity-based approaches to identify the variables governing thermal-bridge behavior [31, 32].

The study also addresses RQ3 and shows that improving wall thermal transmittance without resolving the column junction increases the relative contribution of the thermal bridge to total envelope heat losses. As the thermal performance of the wall improves, unresolved junctions account for a greater share of the remaining thermal penalty. This result reinforces the need to evaluate facade improvement measures together with the behavior of structural thermal bridges rather than considering wall transmittance in isolation. Similar conclusions are reported in previous studies and technical guidance, which indicate that the significance of thermal bridges increases as the rest of the envelope becomes more efficient [32, 54].

From a practical point of view, these findings are especially relevant in internal retrofit scenarios where external insulation systems cannot be applied because of regulatory, architectural, or ownership constraints. In these cases, reinforced concrete columns integrated into facade walls remain a persistent source of thermal discontinuity. The results show that, even under these constraints, some constructive decisions are clearly more effective than others. In particular, the solutions included in Table 7 confirm that the maximum reductions in linear thermal transmittance are associated with configurations that maintain insulation continuity and place the insulation on the exterior side of the column, while also combining adequate thickness and favorable material properties. In this way, Table 7 not only summarizes the best-performing solutions, but also supports the constructive logic derived from the statistical analysis.

Table 7. Solutions achieving the maximum reduction in linear thermal transmittance of the thermal bridge.

Construction typology	Original	Retrofitting
Retrofitting	 Column flush with the exterior	
	 Column flush with the interior	
New construction		

The present interpretation is also consistent with recent studies that emphasize the role of reinforced concrete structural elements as localized sources of thermal discontinuity in building envelopes. In this regard, Evola and Gagliano [55] show, through experimental and numerical analysis, that reinforced concrete pillars may significantly affect heat transfer and envelope thermal performance, even when the rest of the constructive solution performs well. Although that study focuses on a corner pillar and differs from the present case, both studies highlight the need to explicitly consider structural elements when evaluating facade thermal performance. Likewise, Bienvenido-Huertas, Montes, Rubio-Bellido and Canivell [30] confirm the relevance of pillar–wall junctions in warm-climate buildings, which reinforces the practical significance of the present results.

Overall, the study generates practical and applicable knowledge for the design and evaluation of internal facade retrofit strategies in existing buildings with integrated reinforced concrete columns. Rather than focusing on a single constructive detail, it identifies the variables that most strongly influence the thermal penalty of the bridge and establishes an order of relative importance among them. In this way, it supports the optimization of constructive

solutions, the reduction of heat losses, and the improvement of envelope thermal performance under realistic retrofit constraints.

6. Conclusions

This study examines the thermal-bridge effect of reinforced concrete columns embedded in facade walls under internal retrofit conditions. To do so, it analyzes two common facade typologies in the Spanish residential stock through a parametric database of 1,710 simulated solutions and combines two-dimensional finite-element modeling with OLS and Quantile Regression analysis. This approach makes it possible to identify the design variables that most strongly influence the linear thermal transmittance of the junction and to quantify their relative importance.

The results show that insulation continuity around the column is the most influential factor in reducing linear thermal transmittance. In this respect, the study addresses the first research question and confirms that not all construction variables contribute equally to thermal-bridge mitigation. Among the analyzed solutions, continuous insulation placed on the exterior side of the column provides the best thermal performance.

The study also shows that insulation thickness reduces linear thermal transmittance, although its effect is non-linear and displays diminishing returns as thickness increases. This finding is especially relevant in internal retrofit interventions, where thermal improvement must be balanced against space limitations, construction feasibility, and cost. In this sense, the results indicate that ensuring insulation continuity and optimizing the position of the insulation relative to the column may be more effective than simply increasing thickness.

In addition, the study shows that improving wall thermal transmittance without resolving the column junction increases the relative contribution of the thermal bridge to total envelope heat losses. In this way, the study addresses the third research question and highlights the need to integrate the treatment of structural thermal bridges into facade improvement strategies, particularly in better-insulated envelopes, where unresolved junctions account for a greater share of the remaining thermal penalty.

From an applied perspective, the findings provide useful support for decision-making in internal facade retrofit when external insulation systems cannot be used. Although the Spanish case provides the regulatory and constructive reference framework, the main design implications are transferable to similar building stocks in which structural elements embedded in masonry facades interrupt thermal continuity. In this regard, the study offers practical knowledge for the design and evaluation of retrofit strategies, contributes to the optimization of constructive solutions, and supports the reduction of heat losses through integrated facade columns.

The study nevertheless has several limitations. The analysis is restricted to thermal bridges associated with 25 × 25 cm reinforced concrete columns embedded in facades built with either triple hollow ceramic brick coated with single-layer mortar or facing brick. This scope is defined on the basis of two main criteria. First, these configurations represent common constructive solutions in the existing Spanish building stock. Second, extending the analysis to a wider range of variants would have led to an exponential increase in the database, making it necessary to delimit the study. Consequently, only the solutions described in this work are analyzed. Future research should extend the analysis to other facade typologies and column dimensions and should also incorporate additional performance indicators, such as interior surface temperature, condensation risk, and validation or benchmarking procedures. Such developments would provide a broader understanding of thermal bridges and their effect on the overall thermal performance of building envelopes.

Funding

R&D&I Research Project No. GRE22-01A, “Grants for Research Projects and Networks – Category A (Annex X)”, funded by the University of Alicante and carried out under the “Vice-Rectorate for Research’s Internal Programme for the Promotion of R&D&I at the University of Alicante 2023”.

Acknowledgements

The authors acknowledge María López-Pérez for participating in a Collaboration Scholarship in University Departments (academic year 2022–2023) at the University of Alicante, within the framework of which part of this work was developed.

Conflicts of Interest

The authors declare no conflicts of interest.

Appendix A

Table A1. Complete regression results for OLS.

	Unstandardized Coefficients		Std Coef.			95.0% CI for B		Collinearity Statistics	
	B	Std. Error	Beta	t	Sig.	Lower Bound	Upper Bound	Tolerance	VIF
(Intercept)	0.694	0.009		80.036	0.000	0.677	0.711		
Main_wythe_PFB	0.015	0.002	0.036	9.034	0.000	0.012	0.018	1.000	1.000
Position_column_MS_exterior	0.002	0.002	0.004	0.749	0.454	-0.003	0.007	0.692	1.444
Position_column_MS_embedded	0.018	0.002	0.038	8.069	0.000	0.014	0.023	0.707	1.415
Insulation_position_column_outside	-0.102	0.003	-0.204	-36.107	0.000	-0.108	-0.097	0.488	2.049
Brick_encasement_column	-0.008	0.002	-0.016	-3.376	0.001	-0.013	-0.004	0.687	1.455
Cavity_wall	-0.020	0.002	-0.046	-11.658	0.000	-0.023	-0.016	0.998	1.002
Insulation-column ratio_0.5	-0.382	0.003	-0.817	-141.943	0.000	-0.387	-0.376	0.469	2.133
Insulation-column ratio_1.0	-0.442	0.003	-0.947	-164.385	0.000	-0.447	-0.437	0.469	2.133
Insulation-column ratio_1.5	-0.465	0.003	-0.831	-163.842	0.000	-0.470	-0.459	0.604	1.656
Insulation_thickness_cm	-0.014	0.000	-0.184	-46.445	0.000	-0.014	-0.013	0.989	1.011
Insulation_conductivity_x1000	0.003	0.000	0.051	12.814	0.000	0.002	0.003	1.000	1.000

References

[1] F. Déqué, F. Ollivier, J.J. Roux, Effect of 2D modelling of thermal bridges on the energy performance of buildings: Numerical application on the Matisse apartment, Energy and Buildings, 33 (6) (2001) 583-587. doi: https://doi.org/10.1016/S0378-7788(00)00128-6.

[2] T.G. Theodosiou, A.M. Papadopoulos, The impact of thermal bridges on the energy demand of buildings with double brick wall constructions, Energy and Buildings, 40 (11) (2008) 2083-2089. doi: https://doi.org/10.1016/j.enbuild.2008.06.006.

[3] G. Evola, G. Margani, L. Marletta, Energy and cost evaluation of thermal bridge correction in Mediterranean climate, Energy and Buildings, 43 (9) (2011) 2385-2393. doi: https://doi.org/10.1016/j.enbuild.2011.05.028.

[4] H. Ge, V.R. McClung, S. Zhang, Impact of balcony thermal bridges on the overall thermal performance of multi-unit residential buildings: A case study, Energy and Buildings, 60 (2013) 163-173. doi: https://doi.org/10.1016/j.enbuild.2013.01.004.

[5] S. Kotti, D. Teli, P.A.B. James, Quantifying Thermal Bridge Effects and Assessing Retrofit Solutions in a Greek Residential Building, Procedia Environmental Sciences, 38 (2017) 306-313. doi: https://doi.org/10.1016/j.proenv.2017.03.084.

[6] Ministerio de Vivienda, Real Decreto 314/2006, de 17 de marzo, por el que se aprueba el Código Técnico de la Edificación, Boletín Oficial del Estado (BOE), España, 2006. Available online: https://www.boe.es/eli/es/rd/2006/03/17/314/con.

[7] Ministerio de Vivienda, Documento básico de ahorro de energía (DB HE), Código Técnico de la Edificación (CTE), Online, 2006. Available online: https://www.codigotecnico.org/pdf/Documentos/HE/DBAnteriores/DBHE_200602.pdf.

[8] Ministerio de Fomento, Documento de Apoyo al Documento Básico Ahorro de Energía (DA DB-HE / 3). Puentes térmicos, Código Técnico de la Edificación (CTE), Online, 2014. Available online: https://www.codigotecnico.org/pdf/Documentos/HE/DA-DB-HE-3_Puentes_termicos.pdf.

[9] Ministerio de Transportes, Movilidad y Agenda Urbana, Documento básico de ahorro de energía con comentarios del MITMA, Código Técnico de la Edificación (CTE), Spain, 2022. Available online: https://www.codigotecnico.org/pdf/Documentos/HE/DBHE.pdf.

[10] Presidencia del Gobierno, Real Decreto 2429/1979, de 6 de julio, por el que se aprueba la norma básica de edificación NBE-CT-79, sobre condiciones térmicas en los edificios, Boletín Oficial del Estado (BOE), España, 1979. Available online: https://www.boe.es/eli/es/rd/1979/07/06/2429.

[11] INE, Instituto Nacional de Estadística. (2011). Censo de Población y Viviendas de 2011 Instituto Nacional de Estadística (INE). Available online: https://www.ine.es/censos2011_datos/cen11_datos_resultados.htm.

[12] Ministerio de Transportes, Movilidad y Agenda Urbana. (2022). 1. Total de viviendas por comunidades autónomas y provincias Ministerio de Transportes, movilidad y agenda urbana. Available online: https://apps.fomento.gob.es/BoletinOnline2/?nivel=2&orden=33000000.

[13] D. Curto, V. Franzitta, A. Guercio, P. Martorana, FEM analysis: A review of the most common thermal bridges and their mitigation, Energies, 15 (7) (2022) 14. doi: https://doi.org/10.3390/en15072318.

[14] A.E. Saied, C. Maalouf, T. Bejat, E. Wurtz, Slab-on-grade thermal bridges: A thermal behavior and solution review, Energy and Buildings, 257 (2022) 111770. doi: https://doi.org/10.1016/j.enbuild.2021.111770.

[15] Jefatura del Estado, Ley 38/1999, de 5 de noviembre, de Ordenación de la Edificación., Boletín Oficial del Estado (BOE), España, 1999. Available online: https://www.boe.es/eli/es/l/1999/11/05/38/con.

[16] Jefatura del Estado, Real Decreto-ley 8/2011, de 1 de julio, de medidas de apoyo a los deudores hipotecarios, de control del gasto público y cancelación de deudas con empresas y autónomos contraídas por las entidades locales, de fomento de la actividad empresarial e impulso de la rehabilitación y de simplificación administrativa, Boletín Oficial del Estado (BOE), 2011. Available online: https://www.boe.es/eli/es/rdl/2011/07/01/8/con.

[17] Jefatura del Estado, Real Decreto-ley 19/2021, de 5 de octubre, de medidas urgentes para impulsar la actividad de rehabilitación edificatoria en el contexto del Plan de Recuperación, Transformación y Resiliencia, Boletín Oficial del Estado (BOE), España, 2021. Available online: https://www.boe.es/eli/es/rdl/2021/10/05/19.

[18] Jefatura del Estado, Ley 10/2022, de 14 de junio, de medidas urgentes para impulsar la actividad de rehabilitación edificatoria en el contexto del Plan de Recuperación, Transformación y Resiliencia, Boletín Oficial del Estado (BOE), España, 2022. Available online:

https://www.boe.es/eli/es/l/2022/06/14/10.

[19] Ministerio de Industria, Energía y Turismo, Resolución de 25 de septiembre de 2013, de la Secretaría de Estado de Energía, por la que se publica la de 25 de junio de 2013, del Consejo de Administración del Instituto para la Diversificación y Ahorro de la Energía, por la que se establecen las bases reguladoras y convocatoria del programa de ayudas para la rehabilitación energética de edificios existentes del sector residencial (uso vivienda y hotelero), Boletín Oficial del Estado (BOE), España, 2013. Available online: https://www.boe.es/eli/es/res/2013/09/25/(1).

[20] Ministerio de Industria, Energía y Turismo, Resolución de 28 de abril de 2015, del Instituto para la Diversificación y el Ahorro de la Energía, por la que se publica la Resolución de 24 de marzo de 2015, del Consejo de Administración, por la que se modifican las bases reguladoras y convocatoria del programa de ayudas para la rehabilitación energética de edificios existentes del sector residencial (uso vivienda y hotelero), Boletín Oficial del Estado (BOE), España, 2015. Available online: https://www.boe.es/eli/es/res/2015/04/28/(1).

[21] Ministerio de Energía, Turismo y Agenda Digital, Resolución de 14 de diciembre de 2017, del Instituto para la Diversificación y Ahorro de la Energía, por la que se publica la Resolución de 6 de marzo de 2017, del Consejo de Administración, por la que se establecen las bases reguladoras de segunda convocatoria del programa de ayudas para actuaciones de rehabilitación energética de edificios existentes, Boletín Oficial del Estado (BOE), España, 2017. Available online: https://www.boe.es/eli/es/res/2017/12/14/(2).

[22] Ministerio para la Transición Ecológica y el Reto Demográfico, Real Decreto 737/2020, de 4 de agosto, por el que se regula el programa de ayudas para actuaciones de rehabilitación energética en edificios existentes y se regula la concesión directa de las ayudas de este programa a las comunidades autónomas y ciudades de Ceuta y Melilla, Boletín Oficial del Estado (BOE), España, 2020. Available online: https://www.boe.es/eli/es/rd/2020/08/04/737.

[23] Ministerio de Transportes, Movilidad y Agenda Urbana, Real Decreto 853/2021, de 5 de octubre, por el que se regulan los programas de ayuda en materia de rehabilitación residencial y vivienda social del Plan de Recuperación, Transformación y Resiliencia, Boletín Oficial del Estado (BOE), España, 2021. Available online: https://www.boe.es/eli/es/rd/2021/10/05/853.

[24] Ministerio para la Transición Ecológica y el Reto Demográfico, Real Decreto 691/2021, de 3 de agosto, por el que se regulan las subvenciones a otorgar a actuaciones de rehabilitación energética en edificios existentes, en ejecución del Programa de rehabilitación energética para edificios existentes en municipios de reto demográfico (Programa PREE 5000), incluido en el Programa de regeneración y reto demográfico del Plan de rehabilitación y regeneración urbana del Plan de Recuperación, Transformación y Resiliencia, así como su concesión directa a las comunidades autónomas, Boletín Oficial del Estado (BOE), España, 2021. Available online: https://www.boe.es/eli/es/rd/2021/08/03/691.

[25] Ministerio de Transportes, Movilidad y Agenda Urbana. (2022). 2.6. Número de aprobaciones definitivas. Planes estatales y planes autonómicos Ministerio de Transportes, movilidad y agenda urbana. Available online: https://apps.fomento.gob.es/BoletinOnline2/?nivel=2&orden=31000000.

[26] F. Cappelletti, A. Gasparella, P. Romagnoni, P. Baggio, Analysis of the influence of installation thermal bridges on windows performance: The case of clay block walls, Energy and Buildings, 43 (6) (2011) 1435-1442. doi: https://doi.org/10.1016/j.enbuild.2011.02.004.

[27] F. Sierra, J. Bai, T. Maksoud, Impact of the simplification of the methodology used to assess the thermal bridge of the head of an opening, Energy and Buildings, 87 (2015) 342-347. doi: https://doi.org/10.1016/j.enbuild.2014.11.049.

[28] N. Arias Jiménez, A. Bobadilla Moreno, Evaluación experimental y análisis de la mejora con aislamiento para el caso del puente térmico en el frente de forjado, Informes de la Construcción, 69 (546) (2017) e188. doi: https://doi.org/10.3989/ic.15.151.

[29] M.J. Romero, F. Aguilar, P.G. Vicente, Analysis of design improvements for thermal bridges formed by double-brick façades and intermediate slabs for nZEB residential buildings in Spain, Journal of Building Engineering, 44 (2021) 103270. doi: https://doi.org/10.1016/j.jobe.2021.103270.

[30] D. Bienvenido-Huertas, M.V. Montes, C. Rubio-Bellido, J. Canivell, The effect of thermal bridge junctions between pillars and walls in the energy demand of buildings in warm climate, in: A. Rotaru (Ed.) Critical Thinking in the Sustainable Rehabilitation and Risk Management of the Built Environment, Springer International Publishing, Cham, 2021, pp. 437-448. doi: https://doi.org/10.1007/978-3-030-61118-7_35.

[31] A.B. Larbi, Statistical modelling of heat transfer for thermal bridges of buildings, Energy and Buildings, 37 (9) (2005) 945-951. doi: https://doi.org/10.1016/j.enbuild.2004.12.013.

[32] A. Capozzoli, A. Gorrino, V. Corrado, A building thermal bridges sensitivity analysis, Applied Energy, 107 (2013) 229-243. doi: https://doi.org/10.1016/j.apenergy.2013.02.045.

[33] Instituto Eduardo Torroja, Catálogo de elementos constructivos del CTE, Ministerio de Vivienda, España, 2010. Available online: https://www.codigotecnico.org/pdf/Programas/CEC/CAT-EC-v06.3_marzo_10.pdf.

[34] International Organization for Standardization, ISO 10456:2007 Building materials and products — Hygrothermal properties — Tabulated design values and procedures for determining declared and design thermal values, AENOR, Madrid, 2012. Available online: https://tienda.aenor.com/p/norma-iso-10456-2007-040966.

[35] Ministerio de Transportes, Movilidad y Agenda Urbana, Documento de Apoyo al Documento Básico Ahorro de Energía (DA DB-HE / 1). Cálculo de parámetros característicos de la envolvente, Código Técnico de la Edificación (CTE), Online, 2020. Available online: https://www.codigotecnico.org/pdf/Documentos/HE/DA_DB-HE-1_Calculo_de_parametros_caracteristicos_de_la_envolvente.pdf.

[36] International Organization for Standardization, UNE-EN ISO 6946. Building components and building elements. Thermal resistance and thermal transmittance. Calculation methods (ISO 6946:2017, Corrected version 2021-12), AENOR, Madrid, 2021. Available online: https://tienda.aenor.com/p/norma-une-en-iso-6946-2021-n0065066.

[37] C. Huizenga, D. Arasteh, C. Curcija, R. Mitchel, C. Kohler, E. Finlayson, L. Zhu, S. Czarnecki, S. Vidanovic, K. Zelenay, THERM finite element simulator, in, Lawrence Berkeley National Laboratory, California, 2022. Available online: https://windows.lbl.gov/software/therm.

[38] Autodesk, Autocad, in, Autodesk, California, 2022. Available online: https://www.autodesk.com/company.

[39] G. Campos Gordillo. (2021). CTE library for Therm. Available online: https://ecoeficiente.es/libreria-cte-para-therm/.

[40] IBM Corp., IBM SPSS Statistics for Windows, in, Armonk, Nueva York, 2016. Available online: https://www.ibm.com/support/pages/how-cite-ibm-spss-statistics-or-earlier-versions-spss.

[41] M. Korobov, Explaining behavior of Machine Learning models with eli5 library, in: Computer Science, EuroPython, On line, 2017. doi: https://doi.org/10.5446/33771.

[42] J.W. Johnson, J.M. Lebreton, History and Use of Relative Importance Indices in Organizational Research, Organizational Research Methods, 7 (3) (2004) 238-257. doi: https://doi.org/10.1177/1094428104266510.

[43] U. Groemping, Relative importance for linear regression in R: The package relaimpo, Journal of Statistical Software, 17 (1) (2006) 1-27. doi: https://doi.org/10.18637/jss.v017.i01.

[44] J.W. Tukey, Exploratory data analysis, Addison-Wesley Pub. Co., New York, 1977.

[45] R. Koenker, G. Bassett, Regression Quantiles, Econometrica, 46 (1) (1978) 33-50. doi: https://doi.org/10.2307/1913643.

[46] R. Koenker, Quantile Regression, Cambridge University Press, Cambridge, 2005. doi: https://doi.org/10.1017/CBO9780511754098.

[47] M. Buchinsky, Recent advances in quantile regression models: A practical guideline for empirical research, The Journal of Human Resources, 33 (1) (1998) 88-126. doi: https://doi.org/10.2307/146316.

[48] R. Koenker, J.A.F. Machado, Goodness of Fit and Related Inference Processes for Quantile Regression, Journal of the American Statistical Association, 94 (448) (1999) 1296-1310. doi: https://doi.org/10.1080/01621459.1999.10473882.

[49] D.C. Montgomery, E.A. Peck, G.G. Vining, Introduction to Linear Regression Analysis, 5th ed., John Wiley & Sons Inc., New Jersey, 2012.

[50] X. Yan, X. Gang-Su, Linear Regression Analysis: Theory and Computing, World Scientific Publishing Company Pte. Limited, Singapore, 2009.

[51] T.S. Breusch, A.R. Pagan, A simple test for heteroscedasticity and random coefficient variation, Econometrica, 47 (5) (1979) 1287-1294. doi: https://doi.org/10.2307/1911963.

[52] D. Kleinbaum, L. Kupper, A. Nizam, E. Rosenberg, Applied regression analysis and other multivariable methods, 5th ed., Cengage Learning, Boston, 2013.

[53] S. Chatterjee, J.S. Simonoff, Handbook of Regression Analysis, John Wiley & Sons Inc., New Jersey, 2013.

[54] P.G. Schild, P. Blom, Good practice guidance on thermal bridges and construction details - Part 1: Principles, in, Pan European, 2010, pp. 10. Available online: https://www.buildup.eu/en/node/8239.

[55] G. Evola, A. Gagliano, Experimental and Numerical Assessment of the Thermal Bridging Effect in a Reinforced Concrete Corner Pillar, 14 (2) (2024) 378. doi: https://doi.org/10.3390/buildings14020378.